

# A Probabilistic Approach for Alignment with Human Comparisons

Junyu Cao

McCombs School of Business, University of Texas at Austin, junyu.cao@mcombs.utexas.edu

Mohsen Bayati

Graduate School of Business, Stanford University, bayati@stanford.edu

A growing trend involves integrating human knowledge into learning frameworks, leveraging subtle human feedback to refine AI models. Despite these advances, no comprehensive theoretical framework describing the specific conditions under which human comparisons improve the traditional supervised fine-tuning process has been developed. To bridge this gap, this paper studies the effective use of human comparisons to address limitations arising from noisy data and high-dimensional models. We propose a two-stage “Supervised Fine Tuning+Human Comparison” (SFT+HC) framework connecting machine learning with human feedback through a probabilistic bisection approach. The two-stage framework first learns low-dimensional representations from noisy-labeled data via an SFT procedure, and then uses human comparisons to improve the model alignment. To examine the efficacy of the alignment phase, we introduce a novel concept termed the “label-noise-to-comparison-accuracy” (LNCA) ratio. This paper theoretically identifies the conditions under which the “SFT+HC” framework outperforms pure SFT approach, leveraging this ratio to highlight the advantage of incorporating human evaluators in reducing sample complexity. We validate that the proposed conditions for the LNCA ratio are met in a case study conducted via an Amazon Mechanical Turk experiment.

*Key words:* model alignment, supervised fine-tuning, probabilistic bisection, human-AI interaction.

---

## 1. Introduction

In light of the increasing availability of data, the demand for data-driven algorithmic solutions has surged. Machine learning has emerged as the standard technique for numerous tasks, including natural language processing and computer vision, among others. Its great importance has also been demonstrated across various domains of operations research.

Traditional methodologies have predominantly relied on supervised fine-tuning (SFT)<sup>1</sup> techniques by training on noisy-labeled data. A common practice in this context for decision-makers is to directly adopt the output of the best predictor identified by SFT, where the best predictor can be defined by the minimizer of the empirical risk, for example. However, some issues may arise in this approach. One significant challenge emerges from the prevalence of large noise, which can substantially hinder

<sup>1</sup> Supervised fine-tuning is usually used in Large Language Models (LLM). We use supervised fine-tuning and supervised learning interchangeably in this paper.

---

model performance. On the other hand, to mitigate the model misspecification issue, the growing trend toward increasingly complex models may lead to over-parameterization. Over-parameterization presents additional obstacles to the design of efficient and accurate AI systems. In instances where the model exhibits high complexity, such as when the feature dimension is comparable to or exceeds the number of data points, multiple distinct estimators may exhibit seemingly equivalent empirical performance on the training dataset but perform poorly on unseen data, a scenario exacerbated by the inherent under-specification of models (D’Amour et al. 2022). Thus, decision-makers must consider strategic data utilization and refine models to achieve a better performance under different environments.

Recently, an ever-growing number of papers have incorporated human-knowledge into the learning framework (Christiano et al. 2017, Li et al. 2016). Fine-tuning with human feedback has shown a promising direction. For instance, in the design of chatbots, the performance can be adaptively and subsequently improved through the interactions with humans (Ziegler et al. 2019, Ouyang et al. 2022). Ouyang et al. (2022) focuses on fine-tuning approaches to aligning language models, where InstructGPT is fine-tuned with human feedback. In many cases, human evaluators possess domain expertise that goes beyond what can be encoded into a dataset or estimation method. Their deep understanding of the task domain enables them to make informed comparisons that consider context, relevance, and real-world applicability (Deng et al. 2020).

“Thinking is difficult, that’s why most people judge” – Carl Jung. Coming up with an answer is much more difficult than selecting a better answer from pair-wise comparisons. Zhou and Xu (2020) use pair-wise comparisons for story generation; Xu et al. (2023) collect human comparisons over two sampled LLM for the algorithm fine-tuning process. While prior research has showcased remarkable results when integrating human feedback across various applications, it has yet to establish a comprehensive theoretical framework detailing the specific conditions under which human comparison significantly augments the conventional SFT framework. To build on this research trajectory and fill this gap, our paper provides a theoretical framework for the strategic utilization of human comparisons. The primary focus is on addressing the inherent limitations posed by noisy data and the complexities of high-dimensional models. By actively and effectively leveraging human comparisons, we aim to navigate the intricacies of model alignment with the minimal labeling effort.

To connect the machine learning framework with human feedback, we propose a two-stage tractable framework through a probabilistic method. In the first stage, noisy labeled data is fed into the SFT oracle to obtain low-dimensional representations. More specifically, the algorithm can use lasso to select important features from high dimensions or use matrix completion to learn low-rank representations. The second stage employs human comparisons to improve model alignment within this low-dimensional space. Our framework, which utilizes the random utility model to describe

human’s comparison behavior, can incorporate the possibility of false selection in human comparisons. Human may provide incorrect responses, though this noise tends to be substantially lower than that present in labeled data. To accommodate this aspect, we develop a probabilistic bisection approach for the alignment phase. We call this two-stage process as “SFT+HC” framework.

The goal of our paper is to refine the model with a certain precision level and a confidence level using the minimum possible data. The rationale behind this framework design is rooted in the observation that some representation learning techniques, such as autoencoders or deep learning architectures (Zhou and Paffenroth 2017, Akrami et al. 2019), are inherently robust to noisy labels (Li et al. 2021, Taghanaki et al. 2021). These methods aim to capture underlying patterns and structures in the data. Recently, Tsou et al. (2023) show that linear probes trained on the final embedding of pre-trained GPT-2 are surprisingly robust, offering competitive performance and, in some cases, even surpassing the results of full-model fine-tuning, where all weights are updated. In the second stage, we adopt human comparisons instead of human estimations because comparison is a much easier task. Our approach involves sequential design of comparisons and active data acquisition, with the objective of maximizing information and consequently minimizing sample complexity.

To describe the effectiveness of the refinement phase through human comparison, we introduce a new concept called “label-noise-to-comparison-accuracy” (LNCA) ratio. We theoretically characterize the condition for the “SFT+HC” framework performing better than the pure SFT algorithm based on this LNCA ratio. In the large-noise scenario, human evaluators with high selection accuracy can significantly reduce the sample complexity.

### 1.1. Our Contributions

Our contributions are summarized as follows:

- (I) *Modeling*: In a large-noise environment, machine learning models may exhibit fragility, due to the sensitivity to variations in input data and the dynamic nature of their surroundings. To address this challenge, we introduce a novel approach that leverages human comparisons to refine these models. To the best of our knowledge, our study represents the first theoretical attempt aimed at explaining the substantial enhancement of model performance under specific conditions through human comparisons. We present a novel two-stage framework based on a utility model for human comparisons. The model captures a natural phenomena that making distinctions between two options becomes increasingly challenging as they are more similar. Consequently, the accuracy of these comparisons may decrease as the model refines.
- (II) *Theoretical Contributions*:
  - (a) *Probabilistic bisection method*: In the second phase, the decision-maker (DM) sequentially selects two options for human evaluators to compare. The fundamental question at this

stage pertains to the efficient acquisition of valuable information from these human comparisons. To address this challenge, we introduce a probabilistic bisection method, which factors in the uncertainty arising from the accuracy of human comparisons. This method involves two types of actions: the ‘vertical move’ involves human evaluations of the same comparison. Once the algorithm identifies the superior choice with high probability, it proceeds with the ‘horizontal move,’ where the system selects the next pair for comparison. Our objective is to determine identify correct model parameters with a precision of  $\epsilon$  and a confidence level of  $1 - \delta$ . We establish the sample complexity required to achieve these precision and confidence levels.

- (b) *Label-noise-to-comparison-accuracy ratio*: We introduce a novel concept known as the ‘noise-to-human-knowledge ratio,’ which quantifies the relative scale between label noise and human-made comparison accuracy. In essence, when label noise is substantial, but humans can make selections with high accuracy, our two-stage framework outperforms pure Sequential Fine-Tuning (SFT). Specifically, when human selection accuracy deviates from 50%, the sample complexity for the refinement stage is  $O(s \log(1/(\delta\epsilon)))$ . In cases where selection accuracy approaches 50% as the two options become indistinguishable from the true model, the sample complexity increases. We characterize the LNCA ratio conditions under which our SFT+HC framework outperforms pure SFT.
- (III) *Numerical Performance*: We evaluate the LNCA ratio through an empirical study on Amazon Mechanical Turk with a stylized task. The experiment result validates the condition under which “SFT+HC” performs better than pure SFT. Subsequently, we evaluated the performance of our proposed SFT+HC framework and compared it with the pure SFT approach across varying LNCA ratios. Our findings align with our theoretical results, revealing that the superiority of the SFT+HC framework becomes more pronounced under conditions of higher observational noise, higher accuracy of human comparisons, and lower dimensions of important features.

## 1.2. Literature Review

*Alignment and Learning From Human Feedback*. The alignment challenge seeks to synchronize human values with machine learning systems and direct learning algorithms towards the objectives and interests of humans. Machine learning models frequently demonstrate unforeseen deficiencies in their performance when they are implemented in practical contexts, which was identified as *underspecification* (D’Amour et al. 2022). Predictors that perform similarly in the training dataset can exhibit significant variations when deployed in various domains. The presence of ambiguity in a model might result in instability and suboptimal performance in real-world scenarios. Recent papers

have focused on aligning models with human intentions, including training simple robots in simulated environments and Atari games (Christiano et al. 2017, Ibarz et al. 2018), fine-tuning language models to summarize text fine-tuning (Stiennon et al. 2020), optimize dialogue (Jaques et al. 2019). It has been demonstrated that using reinforcement learning from human feedback (RLHF) significantly boosts performance (Bai et al. 2022, Glaese et al. 2022, Stiennon et al. 2020, Dwaracherla et al. 2024). Ouyang et al. (2022) use reinforcement learning from human feedback (Stiennon et al. 2020) to fine-tune GPT-3 to follow a broad class of written instructions. In particular, Zhou and Xu (2020) use pair-wise comparisons for story generation. They find that when comparing two natural language generation (NLG) models, instead of asking human annotator to assign scores separately for samples generated by different models, which resembles the case in the ADEM model (Lowe et al. 2017), it is much easier for human annotators to directly compare one sample generated by the first model against another sample from the second model pairwise and compute the win/loss rate. Zhu et al. (2023) provide reinforcement learning framework with human feedback, specifically, for function approximation for  $K$ -wise comparisons with policy learning as the target. Xu et al. (2023) propose a fine-tuning algorithm by inducing a complementary distribution over the two sampled LLM responses to model human comparison processes, in accordance with the Bradley-Terry model for pairwise comparisons. Different than those above-mentioned work, we provide a theoretical two-stage framework for integrating supervised learning with actively acquired human comparison labels, and characterize the conditions where the two-stage framework outperforms pure SFT algorithms.

*Active Learning.* The core concept behind active learning in machine learning theory is the ability of a model to interactively query a human or an oracle to obtain labels for new data points. Instead of passively learning from a fixed dataset, an active learning algorithm intelligently selects the most informative instances to query for labels. We refer readers to Settles (2009) for a comprehensive review of the active learning algorithm. The literature has concentrated on label complexity to demonstrate the benefit of active learning, which refers to the number of labels requested to attain a specific accuracy. For example, Cohn et al. (1994) demonstrates that active learning can have a substantially lower label complexity than supervised learning in the noiseless binary classification issue. In the presence of noise, other papers focus on the classification problems (Hanneke 2007, Balcan et al. 2006, Hanneke 2011) and regression problems (Sugiyama and Nakajima 2009, Beygelzimer et al. 2009), etc. Though our study has a similar goal of using the fewest possible samples to achieve the target accuracy, we concentrate on the human-AI collaboration framework and try to reduce the sample complexity of human comparisons.

*Data-driven Decision Making and Human in the Loop.* A large body of recent literature on operations research or operations management studied how to effectively utilize data to improve their decisions, including pricing, assortment, recommendation, etc. Motivated by the observation

that human may sometimes have “private” information which an algorithm does not have access to that can improve performance, [Balakrishnan et al. \(2022\)](#) examined new theory that describes algorithm overriding behavior. They designed and experimentally tested feature transparency as an implementable approach that can help people better identify and use their private information. [Ibrahim et al. \(2021\)](#) studied how to address the shared information problem between humans and algorithms in a setting where the algorithm makes the final decision using the human’s prediction as input. [Dietvorst et al. \(2018, 2015\)](#) study algorithm aversion phenomenon where people often fail to use algorithms after learning that they are imperfect, though evidence-based algorithms consistently outperform human forecasters. Other papers study Human-AI collaboration on a large variety of topics ([Bastani et al. 2021](#), [Wu et al. 2022](#), [Deng et al. 2020](#)), including ride-hailing ([Benjaafar et al. 2022](#)) and healthcare ([Reverberi et al. 2022](#)), etc.

*Probabilistic Bisection.* The other related literature, which is independent of the above human-AI ML topics, is probabilistic bisection algorithm ([Horstein 1963](#)). Algorithms utilizing the PBA framework have been employed in several contexts, notably including the task of target localization ([Tsiligkaridis et al. 2014](#)), scanning electron microscopy ([Sznitman et al. 2013](#)), topology estimation ([Castro and Nowak 2008](#)), edge detection ([Golubev and Levit 2003](#)), and value function approximation for optimal stopping problems ([Rodriguez and Ludkovski 2015](#)). From the computational perspective, [Frazier et al. \(2019\)](#) has shown that probabilistic bisection converges almost as quickly as stochastic approximation. In this work, we design the model alignment algorithm by utilizing the probabilistic bisection approach, where the randomness is involved due to the inherent variability in the human judgement process.

### 1.3. Organization of the Paper

The remainder of this paper is organized as follows. Section 2 introduces the model setup. In Section 3, we introduce the model of human comparisons and characterize the sample complexity in a one-dimensional space. In Section 4, we present a two-stage framework which organically integrate SFT and human comparison. We specifically discuss the sample complexity when applying lasso in the first stage. Section 6 shows numerical experiments and managerial insights. Section 7 concludes the paper. Additional proofs and parameter calibrations are provided in the appendices.

## 2. Model

In this section, we introduce our model setup. We first introduce the supervised learning oracle that will be potentially used during the *initial learning stage*, and then present the fine-tuning procedure through human comparisons during the *refinement stage*.

## 2.1. Supervised Learning and Underspecifications

Given data  $\{(X_i, Y_i)\}_{i \leq n}$  where  $X_i \in \mathcal{X}$  and  $Y_i \in \mathcal{Y} \subseteq \mathbb{R}$ , the goal is to learn the true function that is parameterized by  $\boldsymbol{\vartheta}^* \subseteq \mathbb{R}^d$ ,  $h_{\boldsymbol{\vartheta}^*} \in \mathcal{H} : \mathcal{X} \rightarrow \mathcal{Y}$ , where  $\mathcal{H}$  is the function class. Each data point is generated from a stochastic response:

$$Y_i = h_{\boldsymbol{\vartheta}^*}(X_i) + \epsilon_i,$$

where  $\epsilon_i$  is the noise with mean 0 and variance  $\sigma^2$ , where  $\sigma$  could potentially be very large.

We specifically consider a high-dimensional problem that can be represented by low-dimensional manifolds; that is,

$$h_{\boldsymbol{\vartheta}^*}(x) = f_{\boldsymbol{\theta}^*, \varphi(\cdot)}(x),$$

where  $f(\cdot)$  is assumed to be a generalized linear function in  $\boldsymbol{\theta}^*$  and  $\varphi(x)$ . Here  $\boldsymbol{\theta}^* \in \Theta \in \mathbb{R}^s$  is the unknown parameter<sup>2</sup>,  $\varphi(x) \in \mathbb{R}^s$  is the low-dimensional representation of feature  $x$ . It is assumed that  $s \ll d$ . For simplicity, we will remove the subscript  $\varphi(\cdot)$  from  $f$  when it is clear from the context.

We first provide the following two examples as an illustration.

**EXAMPLE 1 (SPARSE LINEAR MODELS).** The parameter  $\boldsymbol{\vartheta}^*$  has nonzero entries in the first  $s$  dimensions and has zero entries in the rest of dimensions. In the linear model,  $f_{\boldsymbol{\vartheta}^*}(x) = \sum_{i=1}^s \vartheta_i^* x_i$ . In this case,  $\boldsymbol{\theta}^* = (\vartheta_1^*, \dots, \vartheta_s^*)$ ,  $\varphi(x) = (x_1, \dots, x_s)$ , and  $f(\cdot)$  is a linear function.

**EXAMPLE 2 (GENERALIZED LOW-RANK MODELS).** In the generalized low-rank models, it is assumed that

$$f_{\boldsymbol{\Theta}^*}(X) = \mu(\langle \boldsymbol{\Theta}^*, xz^\top \rangle) = \mu(x^\top \boldsymbol{\Theta}^* z)$$

where  $\mu(\cdot)$  is the link function,  $\boldsymbol{\Theta}^* \in \mathbb{R}^{d \times d}$  is a low-rank matrix and  $X = xz^\top$ , i.e.,  $\boldsymbol{\Theta}^* = \sum_{i=1}^s \sigma_i u_i v_i^\top$  where  $u_i$  and  $v_i \in \mathbb{R}^d$ . Thus,  $f_{\boldsymbol{\Theta}^*}(X) = \sum_{i=1}^s \sigma_i (x^\top u_i)(v_i^\top z)$ . In this case,  $\varphi(X)$  is the projection of  $X$  onto the low-rank space and  $\boldsymbol{\theta}^*$  is the  $s$ -dimensional vector of singular values.

Suppose  $h_{\boldsymbol{\vartheta}}$  can be estimated through a statistical loss function  $\ell : \mathcal{Y} \times \mathbb{R} \rightarrow \mathbb{R}$ , and the total loss is

$$L_n(h_{\boldsymbol{\vartheta}}) = \sum_{i=1}^n \ell(Y_i, h_{\boldsymbol{\vartheta}}(X_i)).$$

For example,  $\ell$  can represent the squared loss, the regularized squared loss, among others. To deal with the high-dimensional issue, the algorithm learns the low-dimensional representation  $\varphi(x)$  as well as the parameter  $\boldsymbol{\theta}^*$ . To learn the sparse linear models for example, one can apply lasso to select important features and learn the model parameters. To learn the low-rank models, one can use trace regression to learn the low-dimensional representations.

Define  $h_{\hat{\boldsymbol{\vartheta}}_n}$  as the function contained in  $\mathcal{H}$  that minimizes empirical risk  $L_n$ . In the existing literature, it is very common that the decision-maker directly employs the predictor  $h_{\hat{\boldsymbol{\vartheta}}_n}$ . However,

<sup>2</sup>We denote the parameter vector using the bold symbol.



some issues may arise. In high-dimensional problems where significant noise is present, approaches striving to balance the variance-bias trade-off may occasionally diverge from intuitive expectations. We use the following example to illustrate this potential issue.

**EXAMPLE 3.** Consider a linear pricing model with high-dimensional contexts, i.e.,  $Y_i = \vartheta_1 \cdot p_i + \vartheta_2^\top X_i + \epsilon_i$  where  $Y_i$  is the demand,  $p_i$  is the price, and the vector  $X_i$  represents features of product  $i$ , and also assume that  $\vartheta_1 < 0$ . However, in a high-noise regime we may incorrectly estimate a positive value for  $\vartheta_1$ . Please see Appendix B.1 for numerical illustrations.

In Example 3, the positive correlation between price and demand is misinterpreted due to model underspecification. The requirement of  $\vartheta_1 < 0$  should be specified based on human knowledge. In the face of the challenge posed by underspecification within a potentially very noisy environment, we take a critical step towards refinement, which we term “fine-tuning through human comparisons.” Human can do comparisons with a much higher precision. For example, based on the human knowledge, it can be immediately corrected that the demand and the price is negatively correlated. This particular stage comes into play after the output generated by our machine learning pipelines, represented as  $\hat{\varphi}(\cdot)$  and  $\hat{\theta}_0$  (which denotes the estimator of  $\varphi$  and  $\theta$ ), has been produced. During this stage, we focus on enhancing the model within a lower-dimensional space. We move on to the refinement step after the first stage where the kernel function, which provides a low-dimensional representation, has been effectively trained on the noisy-labeled data.

## 2.2. Utility Model of Human Comparisons

In this section, we introduce the human comparison model. Given two potential models  $f_{\theta_1}$  and  $f_{\theta_2}$ , the system asks human to compare and select the better prediction model. If  $f_{\theta_1}$  is more preferable than  $f_{\theta_2}$ , we denote it as  $f_{\theta_1} \succeq f_{\theta_2}$ .

The preference over the model  $f_{\theta}$  is captured by a utility function  $u(\theta)$ , where  $u(\theta)$  depicts the distance between the model parameterized by  $\theta$  and the true model. That is, we assume  $u(\theta) = -d(\theta, \theta^*)$  where  $d(\cdot, \cdot)$  is a distance function. The larger value of utility indicates a better model. The true model parameter  $\theta^*$  achieves the highest utility. For example, it can be the negative two-norm distance, i.e.,  $u(\theta) = -\|\theta - \theta^*\|_2$ . We formally state the assumption about the utility function as follows:

**ASSUMPTION 1 (Utility function).** *Assume  $u(\theta) = -d(\theta, \theta^*)$ , where  $d(\cdot, \cdot)$  is a distance function.*

The utility function is unimodal in each coordinate. That is, for each coordinate  $\theta_i$ , when fixing all other coordinates,  $u(\theta)$  is monotonically increasing when  $\theta_i < \theta_i^*$  and monotonically decreasing when  $\theta_i > \theta_i^*$ . Moreover, the utility gets lower when  $\theta$  gets far away from the true parameter. The utility function can be either bounded or unbounded (e.g., the Euclidean distance). We give another example of the bounded utility function as an illustration.



EXAMPLE 4. Consider  $\theta^* \in \mathbb{R}$ . The prior of the model parameter  $\theta$  is characterized by the probability density function  $v(\cdot)$ . The utility function is  $u(\theta) = -d(\theta, \theta^*) := -|\int_{\theta}^{\theta^*} v(t)dt|$ . In this case, the utility function is bounded.

The comparison between  $f_{\theta_1}$  and  $f_{\theta_2}$  provides information on which side is closer to the true parameter  $\theta^*$ . Define the hyperplane  $H(\theta_1, \theta_2) = \{\theta : d(\theta, \theta_1) = d(\theta, \theta_2)\}$ , and half-space  $H^-(\theta_1, \theta_2) = \{\theta : d(\theta, \theta_1) < d(\theta, \theta_2)\}$  and  $H^+(\theta_1, \theta_2) = \{\theta : d(\theta, \theta_1) > d(\theta, \theta_2)\}$ . The condition  $u(\theta_1) \geq u(\theta_2)$  implies that  $\theta^* \in H^-(\theta_1, \theta_2)$ . Assumption 1 implies that  $H(\theta_1, \theta_2)$  contains a unique point when  $\theta_1$  and  $\theta_2$  are in a one-dimensional space.

REMARK 1. In practice, the comparison between two models can be conducted in various ways. For example, it can be evaluated on a single point with high confidence (either from human's past experience or their observation), denoted as  $\{x, y\}$ . When comparing two models, the one with smaller square loss is more preferred, i.e.,

$$\mathbb{P}(\theta_1 \succeq \theta_2) = \mathbb{P}((y - f_{\theta_1}(x))^2 \leq (y - f_{\theta_2}(x))^2).$$

We will elaborate this process in Section 5.

The overall goal is to find  $\theta$  that achieves near the highest utility, or equivalently, gets close to the true model parameter  $\theta^*$  within a certain precision. Suppose that human's selection process follows a random utility model (RUM). In the process of querying, human's opinion regarding  $f_{\theta}$  is

$$U(\theta) = u(\theta) + \beta_h + \xi,$$

where  $\beta_h$  represents the human bias, and  $\xi$  is the unobserved noise. The human bias  $\beta_h$  can vary between individuals. We assume the noise  $\xi$  follows Gumbel distribution with parameter  $\gamma$ , which represents the expert level of the human. We say the human makes the correct choice if he selects  $\theta_1$  ( $\theta_2$ ) when  $u(\theta_1)$  ( $u(\theta_2)$ ) is higher than  $u(\theta_2)$  ( $u(\theta_1)$ ). A smaller value of  $\gamma$  corresponds to a higher certainty of the selection correctness. When  $\gamma$  approaches 0, human can always select the better one with almost 100% accuracy.

LEMMA 1 (**Precision**). *For any two models  $f_{\theta_1}$  and  $f_{\theta_2}$ , the probability that human will make the right selection is*

$$\frac{1}{1 + \exp(-|u(\theta_2) - u(\theta_1)|/\gamma)},$$

*which is strictly larger than 1/2.*

Lemma 1 implies that under RUM, the selection accuracy is always higher than 50%, even with the nonzero human bias. Intuitively, the differentiation would become harder when  $\theta_1$  and  $\theta_2$  both get closer to the true parameter. However, how fast it converges to 1/2 when  $\theta_1$  and  $\theta_2$  approach

$\theta^*$  depend on the distance function. Under this probabilistic selection model, we will design the algorithm and investigate the sample complexity. The parameter  $\theta$  may lie in a multi-dimensional space. To illustrate our algorithm, we first describe the one-dimensional human comparison procedure, and then extend to the multi-dimensional scenario.

### 3. One-dimensional Human Comparison

Once the low-dimensional representation  $\hat{\varphi}$  has been established in the initial stage, as detailed in Section 4, we introduce a framework for model alignment through human comparisons. The parameter  $\theta$  may lie in a multi-dimensional space. To illustrate our algorithm, we first describe the one-dimensional human comparison procedure, and then extend to the multi-dimensional scenario.

The primary challenge in designing the framework lies in strategically selecting pairwise comparisons to minimize sample complexity, which bears resemblance to the principles of active learning. In this section, we first discuss the deterministic selection (with 100% accuracy) and then study the probabilistic selection. For the probabilistic selection, we propose an algorithm named Alignment through Probabilistic Bisection (APB) and characterize its sample complexity.

#### 3.1. Deterministic Bisection

We first illustrate the algorithm in a one-dimensional space with 100% selection accuracy. This scenario corresponds to  $\gamma \rightarrow 0$  in RUM. In the one-dimensional case, suppose  $\theta^* \in \Theta \subseteq \mathbb{R}$  and  $|\theta| \leq \beta_\Theta$  for all  $\theta \in \Theta$ .

The overall goal is to use the least samples to find some  $\theta$  such that  $d(\theta, \theta^*) \leq \varepsilon$ . When human is able to select a better model with 100% accuracy, the deterministic bisection algorithm can be utilized to approach the true parameter. The algorithm operates by maintaining a search interval  $[\theta^-, \theta^+]$  that contains the true parameter  $\theta^*$ . The interval is initialized by  $[-\beta_\Theta, \beta_\Theta]$ , and at round  $k$  the center of this interval with respect to the distance  $d(\cdot, \cdot)$  is used as *query point*. Specifically, defining the query point  $\theta_k$  to be the single point in the set  $H(\theta^-, \theta^+)$ , we ask the human to compare utility of two points, denoted by  $c_\Delta^-(\theta_k)$  and  $c_\Delta^+(\theta_k)$ , that have equal distance  $\Delta/2$  from  $\theta_k$  in opposite directions, where  $\Delta$  is called comparison granularity and is a tuning parameter. For example, for the Euclidean distance, at each round  $\theta_k = (\theta^- + \theta^+)/2$ , and  $c_\Delta^-(\theta_k) = \theta_k - \Delta/2$  and  $c_\Delta^+(\theta_k) = \theta_k + \Delta/2$ . If the human selects  $c_\Delta^-(\theta_k)$  then we eliminate the upper half of the search interval by updating  $\theta^+$  to be equal to  $\theta_k$ ; otherwise, we eliminate the bottom half of the search interval by setting  $\theta^-$  to be equal to  $\theta_k$ . After this bisection step, we continue the process by selecting  $\theta_{k+1}$  to be  $H(\theta^-, \theta^+)$  again, and repeat the above till the length of the search interval is below the precision  $\varepsilon$ . The pseudo code for this is presented in Algorithm 1.

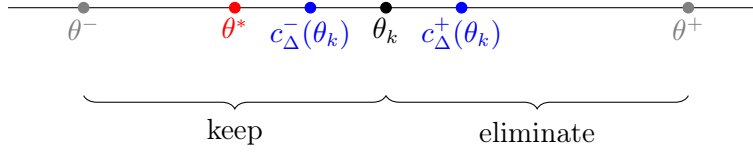


Figure 1: An illustrative example. Among two choices  $c_{\Delta}^{-}(\theta_k)$  and  $c_{\Delta}^{+}(\theta_k)$ ,  $c_{\Delta}^{-}(\theta_k)$  would be selected since it is closer to the true parameter. In this case, the interval  $(\theta_k, \theta^+]$  is eliminated.

---

**Algorithm 1** DB (Deterministic Bisection)

---

- 1: **input**: precision  $\varepsilon$ ; comparison granularity  $\Delta$ ;  $k = 0$ ;  $\theta_k = 0$ ;  $\theta^+ = \beta_{\Theta}$ ;  $\theta^- = -\beta_{\Theta}$ ;
  - 2: **repeat**
  - 3:   Ask human to evaluate  $c_{\Delta}^{-}(\theta_k)$  and  $c_{\Delta}^{+}(\theta_k)$
  - 4:   **if**  $c_{\Delta}^{+}(\theta_k)$  is chosen **then**
  - 5:      $\theta^- = \theta_k$ ;
  - 6:   **else**  $\theta^+ = \theta_k$ ;
  - 7:   **end if**
  - 8:    $k = k + 1$ ;  $\theta_k = H(\theta^-, \theta^+)$ ;
  - 9: **until**  $d(\theta^+, \theta^-) \leq \varepsilon$ .
- 

PROPOSITION 1. *Suppose human makes the selection with 100% accuracy ( $\gamma \rightarrow 0$ ). Fix  $\varepsilon > 0$ . After  $O(\log_2(\frac{\beta_{\Theta}}{\varepsilon}))$  rounds, Algorithm 1 reaches a point  $\theta_k$  such that  $d(\theta_k, \theta^*) \leq \varepsilon$ .*

However, the deterministic model of human selection described above exhibits two significant limitations: firstly, in practical scenarios, humans may not always be able to identify the correct choice, implying that  $\gamma > 0$ ; secondly, the accuracy of human selections is influenced by the comparison granularity  $\Delta$ . To address these concerns, we introduce a more general probabilistic model in the following subsection.

### 3.2. Probabilistic Bisection

First, we enrich the model to capture the probabilistic nature of human comparisons by noting that, in the RUM, when  $\gamma$  is strictly positive, human's selection is random with certain distribution that favors the correct answer, parameterized by  $\gamma$ . Precisely, Lemma 1 indicates that human will select  $c_{\Delta}^{-}(\theta)$  with probability

$$p_{\gamma}^{-}(\theta) := \left[ 1 + \exp \left\{ \frac{u(c_{\Delta}^{+}(\theta)) - u(c_{\Delta}^{-}(\theta))}{\gamma} \right\} \right]^{-1},$$

and selects  $c_{\Delta}^{+}(\theta)$  with probability  $p_{\gamma}^{+}(\theta)$  equal to  $1 - p_{\gamma}^{-}(\theta)$ .

We note that, in the above equation, the selection probability depends on the comparison granularity. This dependence, naturally captures difficulty of the selection for the human. Specifically,

when  $\Delta$  is too small,  $c_{\Delta}^{-}(\theta)$  and  $c_{\Delta}^{+}(\theta)$  converge to each other, hence  $p_{\gamma}^{-}(\theta)$  and  $p_{\gamma}^{+}(\theta)$  converge to  $1/2$ , representing the difficulty of distinguishing between too highly similar choices. On the other hand, when  $\Delta$  is too large, one expects the selection to become difficult as well as both options are far away from  $\theta^*$ . This can be captured for example when the distance function converges to a finite value for far away points from  $\theta^*$  as in Example 4. In this case,  $p_{\gamma}^{-}(\theta)$  and  $p_{\gamma}^{+}(\theta)$  could also converge to  $1/2$  (see Example 5). In the remaining of the paper, for brevity, we do not include  $\Delta$  in the notations  $p_{\gamma}^{-}(\theta)$  and  $p_{\gamma}^{+}(\theta)$ .

EXAMPLE 5. Consider  $u(\theta) = -\frac{1}{1+\exp(-|\theta|)}$  with the highest utility achieved at  $\theta = 0$ . When  $\Delta$  is too large, both  $u(c_{\Delta}^{+}(\theta))$  and  $u(c_{\Delta}^{-}(\theta))$  are close to  $-1$  even  $\theta$  is far away from  $0$ , and thus  $p_{\gamma}^{-}(\theta)$  and  $p_{\gamma}^{+}(\theta)$  are both close to  $1/2$ .

DEFINITION 1 (( $\varepsilon, \delta$ )-ALIGNMENT PROBLEM). Let  $\varepsilon > 0$  denote the precision level and  $\delta > 0$  represent the confidence level. The ( $\varepsilon, \delta$ )-alignment problem aims to identify a  $\theta$  such that  $\mathbb{P}(d(\theta, \theta^*) \leq \varepsilon) \geq 1 - \delta$ .

Our objective is to solve the ( $\varepsilon, \delta$ )-alignment problem with small sample complexity. The algorithm design is inspired by the probabilistic bisection developed in Frazier et al. (2019). While their work primarily focuses on the analysis of convergence rates, our emphasis is on conducting a sample complexity analysis for an algorithm designed to terminate when both the precision level and confidence level criteria are met.

If  $\theta < \theta^*$ , then  $p_{\gamma}^{-}(\theta) < 1/2$  and  $p_{\gamma}^{+}(\theta) > 1/2$ ; vice versa. We introduce some notation for simplicity. Let  $Y(\theta)$  denote the selection:  $Y(\theta) = c_{\Delta}^{-}(\theta)$  with probability  $p_{\gamma}^{-}(\theta)$  and  $Y(\theta) = c_{\Delta}^{+}(\theta)$  with probability  $p_{\gamma}^{+}(\theta)$ . Define  $\tilde{Z}(\theta) = 2 \cdot \mathbf{1}(Y(\theta) = c_{\Delta}^{+}(\theta)) - 1$ , so that  $\tilde{Z}(\theta) = 1$  if  $Y(\theta) = c_{\Delta}^{+}(\theta)$  (so that we believe  $\theta^*$  more likely to be to the right of  $\theta$ ) and  $\tilde{Z}(\theta) = -1$  if  $Y(\theta) = c_{\Delta}^{-}(\theta)$  (so that we believe  $\theta^*$  more likely to be to the left of  $\theta$ ). Note that we have  $\tilde{Z}(\theta) = 1$  with probability  $p_{\gamma}^{+}(\theta)$ . Also, define

$$\tilde{p}(\theta) = \begin{cases} \mathbb{P}(\tilde{Z}(\theta) = 1), & \text{if } \theta \leq \theta^* \\ \mathbb{P}(\tilde{Z}(\theta) = -1), & \text{if } \theta > \theta^* \end{cases},$$

so that  $\tilde{p}(\theta)$  is the probability that  $\tilde{Z}(\theta)$  correctly indicates the direction of the root  $\theta^*$  from  $\theta$ .

Figure 2 shows the structure of introducing our main algorithm. The general idea of the Algorithm APB is described as follows. There are two types of moves: the *horizontal moves* and the *vertical moves*. For any fixed  $\theta$ , we ask human to repeatedly evaluate  $c_{\Delta}^{-}(\theta)$  and  $c_{\Delta}^{+}(\theta)$ . We refer this as the vertical moves. Once the vertical stopping criteria is satisfied, the algorithm decides the next  $\theta$  to evaluate according to the updated distribution. We call this step as the horizontal moves. The horizontal moves continue until the horizontal stopping criteria is satisfied. In the following two sections, we discuss horizontal moves and vertical steps, as well as the stopping criteria, in sequence. Then we introduce the two-stage Human-AI collaboration framework for multiple dimensions in Section 4 and practical implementations in Section 5.

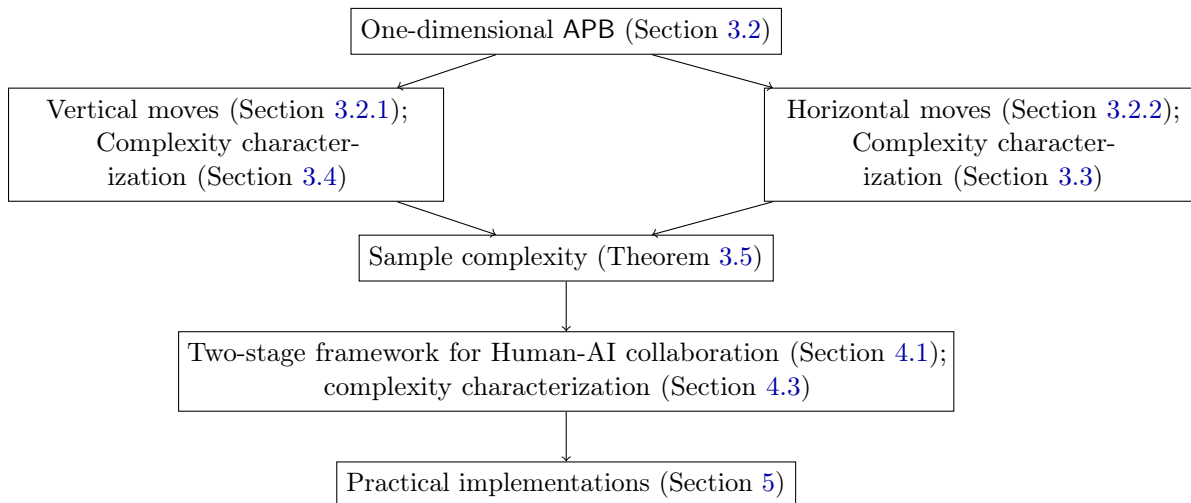


Figure 2: Roadmap for introducing 2.

**3.2.1. Vertical moves** Fix some  $\theta$ . Repeatedly, we ask human evaluations of the query point  $\theta$ , achieved through comparisons of  $c_{\Delta}^+(\theta)$  and  $c_{\Delta}^-(\theta)$ . We observe a sequence of signs  $\{\tilde{Z}_i(\theta)\}_i$ . If  $\theta < \theta^*$ , then the expectation  $\mathbb{E}[\tilde{Z}_i(\theta)] = 2\tilde{p}(\theta) - 1 > 0$ ; if  $\theta > \theta^*$ , then the expectation  $\mathbb{E}[\tilde{Z}_i(\theta)] = 1 - 2\tilde{p}(\theta) < 0$ . From the response  $\tilde{Z}_i(\theta)$ , we define the simple random walk  $S(\theta) = \{S_m(\theta) : m \geq 0\}$  with  $S_0(\theta) = 0$  and  $S_m(\theta) = \sum_{i=1}^m \tilde{Z}_i(\theta)$  for  $m \geq 1$ . Sequential test of power one indicates whether the drift  $\omega$  of a random walk satisfies the hypothesis  $\omega < 0$  versus  $\omega > 0$ .

Define the stopping time  $\tau_1^\uparrow(\theta) = \inf\{m \in \mathbb{N} : |S_m(\theta)| \geq \tilde{h}_m\}$  where  $\{\tilde{h}_m\}_m$  is a positive sequence. Here “ $\uparrow$ ” ( $\rightarrow$ ) represents “vertical” (horizontal, respectively). The test decides that  $\theta < \theta^*$  if  $S_{\tau_1^\uparrow(\theta)}(\theta) \geq \tilde{h}_{\tau_1^\uparrow(\theta)}$ , that  $\theta > \theta^*$  if  $S_{\tau_1^\uparrow(\theta)}(\theta) \leq -\tilde{h}_{\tau_1^\uparrow(\theta)}$  and the test does not make a decision if  $\tau_1^\uparrow(\theta) = \infty$ .

Assume now that the algorithm queries at some point  $\theta_k \neq \theta^*$  at the  $(k+1)^{th}$  iteration. We then observe a random walk with  $m^{th}$  term  $S_{k,m} = S_{k,m}(\theta_k) = \sum_{i=1}^m Z_{k,i}(\theta_k)$  until we reach the end of the power-one test. Define the new signal

$$Z_k(\theta_k) = \begin{cases} +1, & \text{if } S_{k,\tau_1^\uparrow(\theta_k)} > 0, \\ -1, & \text{if } S_{k,\tau_1^\uparrow(\theta_k)} < 0. \end{cases}$$

LEMMA 2. Define  $\tilde{h}_m = (2m(\ln(m+1) - \ln \eta))^{1/2}$ . On the event  $\theta_k > \theta^*$ ,  $\mathbb{P}(Z_k(\theta_k) = +1 | \theta_k) \leq \eta/2$ . On the event  $\theta_k < \theta^*$ ,  $\mathbb{P}(Z_k(\theta_k) = -1 | \theta_k) \leq \eta/2$ . That is, the detection accuracy  $p(\theta)$  when the vertical move stops is bounded by  $p(\theta) \geq 1 - \eta/2$ .

Lemma 2 states that the detection accuracy is lower bounded by  $p_c := 1 - \eta/2$  where the accuracy can be chosen through the selection of  $\eta$ . As  $\theta$  approaches  $\theta^*$ , the differentiation between choices becomes increasingly challenging because the drift tends to diminish, potentially requiring more steps in the testing process. However, it is crucial to remember that our objective is to locate a  $\theta$  such that  $|\theta - \theta^*| \leq \varepsilon$  with a confidence level of  $1 - \delta$ . In the vicinity of  $\theta^*$ , waiting until  $|S_m(\theta)| \geq \tilde{h}_m$  to

terminate the test may not be necessary. A high volume of queries at a particular point  $\theta_k$  suggests close proximity between  $\theta_k$  and  $\theta$ , making it advisable to consider terminating the test sooner.

Based on this insight, we introduce the stopping time  $\tau^\uparrow(\delta, \varepsilon)$  that is determined by the precision and confidence level. This stopping time regulates the maximum number of queries carried out at a single point as  $\theta$  approaches the local neighborhood of the true parameter (a concept to be elaborated on in Section 3.4). Specifically, as  $\theta$  converges towards  $\theta^*$  within a defined local neighborhood, denoted as  $\{\theta' : d(\theta, \theta') \leq a\}$  for some positive constant  $a$ , surpassing the threshold  $\tau^\uparrow(\delta, \varepsilon)$  signifies the difficulty in distinguishing between the parameters due to their proximity. The algorithm terminates.

**3.2.2. Horizontal moves** Algorithm 2 begins with a prior density  $\rho_0$  on  $[-\beta_\Theta, \beta_\Theta]$  that is positive everywhere. For example,  $\rho_0$  can be chosen as a uniform distribution. Choose some  $p \in (1/2, p_c)$  and let  $q = 1 - p$ . When the algorithm queries at the point  $\theta_k$  to obtain  $Z_k$ , we update the density  $\rho_k$ :

(I) If  $Z_k(\theta_k) = +1$ , then

$$\rho_{k+1}(\theta') = \begin{cases} 2p\rho_k(\theta'), & \text{if } \theta' \geq \theta_k; \\ 2q\rho_k(\theta'), & \text{if } \theta' < \theta_k. \end{cases}$$

(II) If  $Z_k(\theta_k) = -1$ , then

$$\rho_{k+1}(\theta') = \begin{cases} 2q\rho_k(\theta'), & \text{if } \theta' \geq \theta_k; \\ 2p\rho_k(\theta'), & \text{if } \theta' < \theta_k. \end{cases}$$

The next query point  $\theta_{k+1}$  is determined as the median of  $\rho_{k+1}$ . The probability density in the correct side would be increased while the probability density in the wrong side would be reduced. Define  $\tau^\rightarrow(\delta, a)$  as the number of horizontal moves to reach  $a$ -neighborhood of  $\theta^*$  with confidence level  $1 - \delta$  (which will be specified later). That is, parameter  $\theta$  moves to the local  $a$ -neighborhood of  $\theta^*$  with probability at least  $1 - \delta/2$  when the number of steps exceeds  $\tau^\rightarrow(\delta/2, a)$ . The horizontal move stops when the total number of movement reaches  $\tau^\rightarrow(\delta/2, \varepsilon)$  since the precision level  $\varepsilon$  is achieved.

In summary, there are two scenarios:

- (I) If the horizontal move is less than  $\tau^\rightarrow(\delta/2, a)$  (indicating it may not yet reach the local neighborhood of  $\theta^*$  within a distance of  $a$ ), the vertical test stops when it reaches  $\tau_1^\uparrow(\theta)$ . Then it moves to the next query point  $\theta$ ;
- (II) If the horizontal move is more than  $\tau^\rightarrow(\delta/2, a)$  (signifying entry into the local neighborhood of  $\theta^*$  within a distance of  $a$ ):
  - (a) If the vertical move reaches  $\tau^\uparrow(\delta/2, \varepsilon)$  first, the algorithm terminates, having identified a  $\theta$  within the  $\varepsilon$  range of  $\theta^*$ ;
  - (b) Alternatively, if the vertical movement reaches  $\tau_1^\uparrow(\theta)$  first, the vertical test stops and then transitions to the next query point  $\theta$ .

The rationale behind distinguishing between local and non-local scenarios lies in the observation that two distinct situations can result in a significant number of vertical moves: when both compared models are performing well (i.e.,  $\theta_1$  and  $\theta_2$  are close to  $\theta^*$ ), or when both models are performing poorly (i.e.,  $\theta_1$  and  $\theta_2$  are far from  $\theta^*$ ). In the latter scenario, it is imperative that the algorithm does not terminate prematurely, as  $\theta$  has not yet approached  $\theta^*$  sufficiently. Therefore, the stopping criterion  $\tau^\uparrow(\delta, \varepsilon)$  is only applied when  $\theta$  transitions into the local neighborhood of  $\theta^*$ .

Algorithm 2 is described as follows. We initialize the distribution as  $\mu_0$ . Without any historical data,  $\mu_0$  can be initialized as the uniform distribution over the confidence region. Alternatively,  $\mu_0$  can be approximated by the empirical distribution of the estimator from the bootstrap method applying to the first phase. At step  $k$ , the algorithm tests  $\theta_k$  by collecting  $Z_{k,s}(\theta_k)$ . If  $\theta$  is located at the local neighborhood of  $\theta^*$  ( $k \geq \tau^\rightarrow(\delta/2, a)$ ) and the current step label  $s$  is larger than  $\tau^\uparrow(\delta/2, \varepsilon)$ , then the algorithm stops and  $\theta = \theta_k$ . Otherwise, the vertical move stops when  $s$  is larger than  $\tau_1^\uparrow(\theta_k)$ . Once the test on  $\theta_k$  stops, we update prior distribution  $\rho_k$  and select the next  $\theta_{k+1}$  as the median of the updated distribution.

---

**Algorithm 2** APB (Alignment through Probabilistic Bisection)

---

```

1: input: confidence level  $\delta$ , precision  $\varepsilon$ ; initial distribution  $\mu_0$ ; local parameter  $a > 0$ ;  $k = 0$ ;  $\eta$ ;
2: repeat
3:   pick  $\theta_k$  as the median of  $\mu_k$ 
4:    $s = 0$ 
5:   repeat
6:     test  $\theta_k$  by collecting  $Z_{k,s}(\theta_k)$ 
7:      $s = s + 1$ 
8:     if  $k \geq \tau^\rightarrow(\delta/2, a)$  and step  $s$  satisfies stopping criteria  $\tau^\uparrow(\delta/2, \varepsilon)$  then
9:       Algorithm terminates and  $\theta = \theta_k$ 
10:    end if
11:  until vertical step  $s$  satisfies stopping criteria  $\tau_1^\uparrow(\theta_k)$ 
12:   $k = k + 1$ ; update prior distribution  $\rho_k$ 
13: until horizontal step  $k$  satisfies stopping criteria  $\tau^\rightarrow(\delta, \varepsilon)$ 

```

---

### 3.3. Complexity of Horizontal Moves

Let  $T^\uparrow(\theta)$  denote the number of comparisons that are collected at  $\theta$  and  $T^\rightarrow$  denote the number of horizontal moves; let  $T_k^+$  denote the total number of comparisons that are collected after  $k$  horizontal-moves, where “+” denotes both horizontal- and vertical-moves. Note that  $T^\uparrow(\theta)$ ,  $T^\rightarrow$ , and



$T_k^+$  are all random variables. In what follows, we discuss the complexity of vertical and horizontal moves, and characterize its sample complexity.

We first characterize the complexity of horizontal moves. Fix some  $a \in (0, \theta^* + \beta_\Theta)$ . Define three regions:  $A = [-\beta_\Theta, \theta^* - a]$ ,  $B = (\theta^* - a, \theta^*]$ ,  $C = (\theta^*, \beta_\Theta]$ . Define  $T(a) = \inf\{k' \geq 0 : \theta_k \in B \cup C, \forall k \geq k'\}$  to be the time required until the sequence of medians never reenters  $A$ . Let  $\nu_k$  denote the (random) measure corresponding to the conditional posterior distribution, conditional on lying to the left of  $\theta^*$ , so that for any measurable  $D$ ,  $\nu_k(D) = \mu_k(D \cap [-\beta_\Theta, \theta^*]) / \mu_k([-\beta_\Theta, \theta^*])$ . Next, fix  $\Delta \in (0, 1/2)$  and define the stopping time  $\tau(a)$  to be the first time that the conditional mass in  $B$  lies above  $1 - \Delta$  and the median  $\theta_k$  lies to the left of  $\theta^*$ , i.e.,

$$\tau(a) = \inf\{k \geq 0 : \nu_k(B) > 1 - \Delta, \theta_k < \theta^*\}.$$

In line with the approach taken by [Frazier et al. \(2019\)](#) in establishing a connection between  $T(a)$  and  $\tau(a)$ , we present a similar result in Lemma 3.

LEMMA 3. *It holds that*

$$T(a) \leq_{s.t.} \tau(a) + R, \tag{3.1}$$

where  $R$  is a random variable that is independent of  $\tau(a)$  and  $a$ .

From (3.1), to bound  $T(\cdot)$ , we characterize the distribution of  $\tau(\cdot)$ . Algorithm 2 starts with an initial distribution  $\mu_0$ . Without any prior information,  $\mu_0$  can be set as a uniform distribution; otherwise we can use the prior information to update  $\mu_0$ . We first make the following mild assumption regarding the initial prior distribution.

ASSUMPTION 2 (**Prior distribution**). *The initial prior distribution satisfies that  $\mu_0(B) \geq a^\varsigma$  for some  $\varsigma \leq 1$ .*

The uniform distribution satisfies Assumption 2 since  $\mu_0(B) = \mu_0((\theta^* - a, \theta^*]) = a$ . With additional information, the prior distribution would be more centered around the true parameter  $\theta^*$ . Thus,  $\varsigma$  is assumed to be less than or equal to 1. Under this assumption of prior distribution, we analyze the distribution of  $\tau(\cdot)$  in Lemma 4.

LEMMA 4. *Under Assumption 2, by setting  $r = r_2\alpha/(4\varsigma)$ ,*

$$\mathbb{P}(\tau(\omega e^{-rk}) > k/2) \leq e^{-r_2\alpha k/4} \cdot \frac{\theta^*}{\omega^\varsigma} + \beta e^{-r_1 k/2},$$

for some  $r_1, r_2, \alpha > 0$  and any  $\omega > 0$ .

Lemma 4 has shown the light tail distribution of  $\tau(\cdot)$ . For small  $\omega$ , note that  $\omega^\varsigma$  decreases in  $\varsigma$ . That is, when the initial prior distribution is more centered around the true parameter,  $\varsigma$  is smaller and thus the right-hand-side tail distribution is lighter.

We next characterize the complexity of horizontal moves.

**THEOREM 1 (Sample complexity of horizontal moves).** *Under Assumption 2, by setting*

$$\tau^\rightarrow(\delta, \varepsilon) = \max \left\{ \frac{4\zeta(1+\zeta) \log(\frac{8\theta^*}{\delta\varepsilon^\zeta})}{r_2\alpha}, \frac{2\log(8\beta_2/\delta)}{r_1}, \frac{\log(8\beta_2/\delta)}{r_R} \right\}.$$

we have that

$$\mathbb{P}(|\theta_k - \theta^*| \leq \varepsilon) > 1 - \delta, \quad \forall k \geq \tau^\rightarrow(\delta, \varepsilon).$$

Theorem 1 states that after  $\tau^\rightarrow(\delta, \varepsilon)$  horizontal moves,  $\theta_k$  reaches  $\varepsilon$ -neighborhood of the true parameter with probability at least  $1 - \delta$ . The complexity of this process depends on  $\log(1/\delta)$ ,  $\log(1/\varepsilon)$ , and  $\zeta(1+\zeta)$ . When the initial prior distribution is more centered around the true parameter  $\theta^*$ , fewer horizontal moves are needed.

Define the local region of  $\theta^*$  as  $[\theta^* - a, \theta^* + a]$ . We divide the horizontal moves to two phases: Phase I includes all steps until the sequence of medians never reenters  $[-\beta_\Theta, \theta^* - a] \cup [\theta^* + a, \beta_\Theta]$ ; Phase II includes all steps after Phase I. Similar to the definition of  $T(a)$ , we define  $T'(a)$  as the stopping time that the medians never reenters  $A' = [\theta^* + a, \beta_\Theta]$ . Let  $\psi(a)$  be the time required until the sequence of medians never reenters  $A \cup A'$ , i.e.,  $\psi(a) = \max\{T(a), T'(a)\}$ . Proposition 2 provides an upper bound for the expectation of moves outside of  $[\theta^* - a, \theta^* + a]$ .

**PROPOSITION 2.** *The expectation of  $\psi(a)$  is bounded by*

$$\mathbb{E}[\psi(a)] \leq \frac{4\theta^*}{r_2\alpha a} + \frac{4\beta_1}{r_1} + \frac{2\beta_2}{r_R}.$$

### 3.4. Complexity of Vertical Moves

The vertical move has two stopping criteria, depending on whether  $\theta_k$  has moved to the local neighborhood of  $\theta^*$ . If  $\theta_k$  is still outside of the local area, the algorithm would finish the power-one test; otherwise, the algorithm may terminate earlier before stopping the power-one test.

Lemma 5 first characterizes the expected number of queries needed for testing  $\theta$ .

**LEMMA 5 (Power-one test).** *For any  $\theta \neq \theta^*$ ,*

$$\mathbb{E}[\tau_1^\uparrow(\theta)] \leq c_1 |2\tilde{p}(\theta) - 1|^{-2} \ln(|2\tilde{p}(\theta) - 1|^{-1}) + c_2,$$

for some  $c_1, c_2 > 0$ .

Lemma 5 implies that the expected number of vertical moves increases in the order of  $O((2\tilde{p}(\theta) - 1)^{-2})$  when  $\tilde{p}(\theta)$  approaches  $1/2$ . When  $\tilde{p}(\theta)$  is bounded away from  $1/2$ , the expected vertical move is also bounded. Lemma 1 shows that  $\tilde{p}(\theta)$  is strictly larger than  $1/2$  for any  $\theta \neq \theta^*$ , then according to Heine–Borel theorem, there exists  $\delta' > 0$  such that  $\tilde{p}(\theta) > 1/2 + \delta'$  for all  $\theta \in [-\beta_\Theta, \theta^* - a] \cup [\theta^* + a, \beta_\Theta]$  (see the proof of Lemma 7 in Appendix A.1). For the ease of notation, we define the bound of vertical moves

$$\phi(\tilde{p}) = c_1 |2\tilde{p} - 1|^{-2} \ln(|2\tilde{p} - 1|^{-1}) + c_2.$$

The selection accuracy bounded away from  $1/2$  implies that  $\max_{a \leq \|\theta - \theta^*\| \leq \beta_\Theta} \phi(\tilde{p}(\theta))$  is bounded. Thus, we can infer the expected number of steps—comprising both horizontal and vertical movements—outside of  $[\theta^* - a, \theta^* + a]$  as follows.

**PROPOSITION 3 (Sample complexity of Phase I).** *The expected steps outside of  $[\theta^* - a, \theta^* + a]$  is bounded by*

$$\mathbb{E} \left[ \sum_{k=1}^{\psi(a)} T^\uparrow(\theta_k) \mathbf{1}(\|\theta_k - \theta^*\| \geq a) \right] \leq \left( \frac{4\theta^*}{r_2 \alpha a} + \frac{4\beta_1}{r_1} + \frac{2\beta_2}{r_R} \right) \max_{a \leq \|\theta - \theta^*\| \leq \beta_\Theta} \phi(\tilde{p}(\theta)).$$

Proposition 3 highlights that the sample complexity of Phase I hinges on the choice of  $a$  and the span of  $\theta$  from the prior distribution. If  $\beta_\Theta$  is overly expansive, there is a high probability that both selected parameters  $\theta_1$  and  $\theta_2$  are distant from the true parameter. Consequently, the accuracy of human selection may diminish considerably, resembling random selection, as illustrated in Example 5. Thus, by narrowing the range of  $\theta$  based on supplementary information, the sample complexity of Phase I can be notably diminished.

Once Phase I ends,  $\theta_k$  moves to the  $a$ -neighborhood of  $\theta^*$ . In scenarios where both choices are close to  $\theta^*$ , discerning the superior parameter becomes more challenging. Depending on whether the selection accuracy converges towards  $1/2$  as the detected parameter approaches the true parameter, we classify the problem into two cases: 1) The selection accuracy is bounded away from  $1/2$  for all  $\theta \neq \theta^*$ ; 2) the section accuracy approaches  $1/2$ . The second case is harder and requires more delicate analysis. We first characterize the sample complexity for case 1) and then analyze case 2).

For the scenario where  $\tilde{p}$  is bounded away from  $\underline{p} > 1/2$ , combining the bound on the vertical moves (Proposition 3) with the complexity of the horizontal moves (Theorem 1), Theorem 2 characterizes the total sample complexity.

**THEOREM 2 (Sample complexity when  $\underline{p}$  exists).** *If  $\tilde{p}(\theta) \geq \underline{p} > 1/2$  for all  $\theta \in \Theta$ , then the expected samples collected before algorithm termination is*

$$\mathbb{E}[T_{T \rightarrow}^+] \leq \tau^\rightarrow(\delta, \varepsilon) \cdot \phi(\underline{p}) = O(\log(1/(\delta\varepsilon))).$$

Next, we address the more challenging scenario in which the selection accuracy tends towards  $1/2$  as the tested parameter approaches the true parameter.

**3.4.1. When the selection accuracy approaches  $1/2$ .** As the comparison accuracy approaches  $1/2$ , the vertical move (power-one test) requires collecting more samples. The rate at which the vertical sample complexity increases depends on the rate at which the utility changes as  $\theta$  converges to  $\theta^*$ . To account for this effect, we introduce the following assumption.

ASSUMPTION 3. For any  $\theta$  such that  $\|\theta - \theta^*\| \leq a$ , there exists  $\lambda_\Delta > 0$  and  $0 < \kappa \leq 1$  such that

$$|u(c_\Delta^+(\theta)) - u(c_\Delta^-(\theta))| \geq \lambda_\Delta \|\theta - \theta^*\|^\kappa.$$

The parameter  $\kappa$  characterizes the speed of convergence, with a smaller value indicating a faster convergence rate. It is natural to assume  $\kappa \leq 1$  for several reasons. Firstly, human decision-making should not be inferior to learning from a random sample; otherwise, collecting random samples would suffice. We demonstrate this by examining the selection accuracy of learning from a single sample. Suppose the sample  $(x, y)$  is generated from  $y = \theta^*x + \epsilon$  where  $\epsilon \sim \mathcal{N}(0, \sigma^2)$ . When comparing  $\theta + \Delta$  and  $\theta - \Delta$  (without loss of generality, assuming  $\theta < \theta^*$ ),  $\theta + \Delta$  is more preferable than  $\theta - \Delta$  if the residual is smaller. That is, the probability of  $\theta + \Delta$  being better is

$$\begin{aligned} \mathbb{P}(\theta + \Delta \succeq \theta - \Delta) &= \mathbb{P}((\theta^*x + \epsilon - (\theta + \Delta)x)^2 \leq (\theta^*x + \epsilon - (\theta - \Delta)x)^2) \\ &= \mathbb{P}(\epsilon \geq (\theta - \theta^*)|x|) = \frac{1}{2} + \Omega((\theta^* - \theta)|x|). \end{aligned}$$

If we use  $B$  i.i.d. samples, then the probability of  $\theta + \Delta$  being better is  $\frac{1}{2} + \sqrt{B}\Omega((\theta^* - \theta)|x|)$ . The detailed proof is included in Appendix B.2. In instances where evaluation is conducted solely on a random sample,  $\kappa$  is equal to 1. Considering that humans possess additional side information and can make better comparisons, we anticipate  $\kappa$  to be, at most, 1.

LEMMA 6 (**How selection accuracy converges**). Under Assumption 3, it holds that

$$\tilde{p}(\theta) - 1/2 \geq c\|\theta - \theta^*\|^\kappa, \forall \theta \in [\theta^* - a, \theta^* + a],$$

where  $c = \min\{\lambda_\Delta/(8\gamma \ln(2)), 1/(6a)\}$ .

Under Assumption 3,  $\tilde{p}(\theta)$  converges to  $1/2$  with the speed no faster than the linear convergence. Therefore, when  $\theta$  moves to the  $a$ -neighborhood of  $\theta^*$ , the distance between  $\theta$  and  $\theta^*$  can be bounded by  $((\tilde{p}(\theta) - 1/2)/c)^{1/\kappa}$ . In another word, the closeness between  $\tilde{p}(\theta)$  and  $1/2$  implies the closeness between  $\theta$  and  $\theta^*$ . Thus, we can define  $\tau^\uparrow(\delta, \varepsilon)$  as the threshold of the vertical test such that if the vertical move  $T^\uparrow(\theta)$  has reached  $\tau^\uparrow(\delta, \varepsilon)$ , then  $\theta$  is close enough to  $\theta^*$ .

THEOREM 3 (**Vertical moves in Phase II**). Suppose Assumption 3 holds. When  $T^\rightarrow \geq \tau_1^\rightarrow(a, \delta/2)$  and  $T^\uparrow(\theta_{T^\rightarrow}) \geq \tau^\uparrow(\delta/2, \varepsilon)$  where

$$\tau^\uparrow(\delta, \varepsilon) = \max\left\{\tau_0, \frac{8 \log(1/\delta)}{c^2 \varepsilon^{2\kappa}}\right\} = O(\log(1/\delta) \varepsilon^{-2\kappa}),$$

and  $\tau_0 = \{\max s : \tilde{h}_s/s \geq c\varepsilon^\kappa/2\}$  where  $c$  is defined in Lemma 6, then we have

$$\mathbb{P}(\|\theta_{T^\rightarrow} - \theta^*\| \leq \varepsilon) \geq 1 - \delta.$$

When Assumption 3 holds and  $\theta$  moves to the neighborhood of  $\theta^*$ , the sample complexity of the vertical move would not exceed  $O(\varepsilon^{-2\kappa})$  where  $\varepsilon$  is the precision. The vertical sample complexity increases with the value of  $\kappa$ . The faster the selection accuracy converges to  $1/2$ , the harder the selection problem, and thus the higher the vertical sample complexity. In the extreme case where  $\kappa = 0$ ,  $\tilde{p}(\theta)$  is bounded away from  $1/2$  so  $\tau^\uparrow(\delta, \varepsilon)$  is bounded. This conclusion is consistent with what we have in Theorem 2.

### 3.5. Sample Complexity

Combining the sample complexity of horizontal moves and vertical moves, we conclude the total sample complexity of APB.

**THEOREM 4 (Sample complexity of APB).** *Under Assumption 3, the expected number of moves is bounded by*

$$\mathbb{E} \left[ \sum_{k=1}^{T^\rightarrow} T^\uparrow(\theta_k) \right] \leq H(\delta, \varepsilon; a) = \tilde{O}(\varepsilon^{-2\kappa}),$$

where

$$H(\delta, \varepsilon; a) = \left( \frac{4\theta^*}{r_2\alpha a} + \frac{4\beta_1}{r_1} + \frac{2\beta_2}{r_R} \right) \max_{a \leq \|\theta - \theta^*\| \leq \beta_\Theta} \phi(\tilde{p}(\theta)) + \max\{\tau^\rightarrow(\delta, \varepsilon), \tau^\rightarrow(\delta/2, a)\} \tau^\uparrow(\delta/2, \varepsilon).$$

Theorem 4 analyzes the (human) sample complexity in a one-dimensional space, which is in the order of  $\tilde{O}(\varepsilon^{-2\kappa})$ . The horizontal move is in the logarithm order, so the dominant part comes from the vertical moves in the neighborhood of  $\theta^*$ . If human have the ability to differentiate between any two parameters  $\theta_1$  and  $\theta_2$  with probability strictly higher than  $1/2 + \delta'$  as long as  $\theta_1 \neq \theta_2$ , then the total complexity is in the logarithm order of both confidence  $1/\delta$  and precision  $1/\varepsilon$ .

In a  $d$ -dimensional space, if naively refining parameters along each dimension to make the parameter within a  $\varepsilon$ -ball (in  $\ell_p$ -norm), then the total complexity is  $dH(\delta/d, \varepsilon/d^{1/p}; a)$ , which scales as  $\tilde{O}(d^{1+\frac{2\kappa}{p}}/\varepsilon^{-2\kappa})$ . However, in a high-dimensional space,  $d$  can be very large while the true parameter may lie in a low-dimensional manifold. However, in high-dimensional spaces,  $d$  can be significant even though the true parameter may lie within a low-dimensional manifold. In the following section, we explore leveraging a supervised learning oracle to reduce sample complexity.

## 4. Alignment: Human-AI Interaction

In the last section, we discussed the framework of purely using human feedback in a one-dimensional space. In practice, a noisy labeled dataset can usually be acquired easily. A noisy labeled dataset can be potentially utilized for learning the low-dimensional representation  $\varphi(\cdot)$  and thus reducing the complexity of the refining step. In this section, we propose a two-stage framework where the first stage learns the low-dimensional representation using noisy labels and the second stage refines the model using human feedback.

#### 4.1. Two-stage Framework

Suppose the true parameter lies in a  $s$ -dimensional space where  $s \ll d$ . Given confidence  $\delta$  and precision  $\varepsilon$ , we introduce a two-stage framework SFT+HC:

- (I) In Stage 1, the algorithm feeds  $N_1^{HAI}(\delta, \varepsilon)$  noisy labeled data  $(\mathbf{X}, Y)$  to the supervised learning oracle (e.g., Lasso), where  $\mathbf{X} \in \mathbb{R}^{N_1^{HAI} \times d}$  is the design matrix and  $Y$  is the noisy response. At the end, we learn the  $s$ -dimensional embedding  $\varphi(\cdot)$ ;
- (II) In Stage 2, the algorithm asks human to refine the estimator along  $s$  dimensions. This stage requires  $N_2^{HAI}(\delta, \varepsilon)$  data points.

---

#### Algorithm 3 SFT+HC (Supervised Fine-Tuning + Human Comparison)

---

- 1: **input:** confidence level  $\delta$ , precision  $\varepsilon$ ; initial distribution  $\mu_0$ ; local parameter  $a > 0$ ;  $k = 0$ ;  $\eta$ ;
  - 2: **Stage 1:** Learn the embedding  $\varphi(\cdot)$  through SFT oracle trained on data  $(\mathbf{X}, Y)$  with size  $N_1^{HAI}(\delta, \varepsilon)$ ;
  - 3: **Stage 2:** Execute Algorithm 2 (APB) by querying  $N_2^{HAI}(\delta, \varepsilon)$  samples.
- 

The framework design is grounded in the insight that certain representation learning techniques, like autoencoders or deep learning architectures, are inherently robust to noisy labels (Li et al. 2021, Taghanaki et al. 2021). Stage 1 is dedicated to uncovering underlying patterns and structures within the data. Given the effectiveness of human expertise in model refinement, Stage 2 endeavors to enhance model alignment through targeted sample querying. In what follows, we specifically discuss sparse linear models (Example 1), where Stage 1 applies Lasso<sup>3</sup> to select important features.

#### 4.2. Illustration on Linear Models

To demonstrate the sample complexity reduction for the two-stage framework compared to purely trained by supervised learning and provide theoretical justifications, we focus on sparse linear models:

$$Y_i = \langle \boldsymbol{\vartheta}^*, X_i \rangle + \epsilon_i = \langle \boldsymbol{\theta}^*, \varphi(X_i) \rangle + \epsilon_i,$$

where  $\varphi(\cdot)$  projects  $X_i$  to all important features;  $S$  is the index set of all important features; the parameter  $\boldsymbol{\theta}^*$  satisfies that  $|\theta_i^*| \geq \underline{\beta}_\Theta > 0$  for all  $i \in S$ . In the initial stage, we employ Lasso for the selection of significant features, followed by human comparisons for alignment. To assess the sample complexity of our two-stage framework, we will sequentially quantify the size of samples needed for two stages. Firstly, we establish the following standard assumptions for the analysis of Lasso.

**ASSUMPTION 4 (sub-Gaussian noise).** *The observational noise is zero-mean i.i.d. sub-Gaussian with parameter  $\sigma$ .*

<sup>3</sup> OLS and thresholding may serve the same purpose as Lasso.

ASSUMPTION 5. For the random design matrix  $\mathbf{X} \in \mathbb{R}^{n \times d}$  input in the first stage, we assume the following three conditions holds:

- (I) *Mutual incoherence*:  $\max_{j \in S^c} \|(\mathbf{X}_S^\top \mathbf{X}_S)^{-1} \mathbf{X}_S^\top x_j\|_1 \leq \alpha_1$ .
- (II) *Lower eigenvalue*:  $\lambda_{\min}(V_S) \geq \lambda_0 > 0$ , where  $V_S = \frac{1}{n} \mathbf{X}_S^\top \mathbf{X}_S$ .
- (III)  *$\ell_\infty$ -curvature condition*:  $\|Vz\|_\infty \geq \alpha_2 \|z\|_\infty$ , for all  $z \in C_{\alpha'}(S)$ , where  $C_{\alpha'}(S) = \{\Delta \in \mathbb{R}^d \mid \|\Delta_{S^c}\|_1 \leq \alpha' \|\Delta_S\|_1\}$ .

Assumption 5 is standard for the analysis of Lasso. Consider a random design matrix  $\mathbf{X} \in \mathbb{R}^{n \times d}$  with i.i.d.  $\mathcal{N}(0, 1)$  entries for example, we can easily verify that it satisfies mutual incoherence, lower eigenvalue, and  $\ell_\infty$ -curvature condition. Under Assumption 4 and 5 and based on Corollary 7.22 in [Wainwright \(2019\)](#), we derive the following theorem that bounds the infinite distance between vector  $\hat{\theta}_S$  and  $\theta_S^*$ .

THEOREM 5. Under Assumption 4 and 5, suppose that we solve the Lagrangian Lasso with regularization parameter

$$\lambda_n = \frac{2C\sigma}{1 - \alpha_1} \left\{ \sqrt{\frac{2 \log(d-s)}{n}} + \zeta \right\}$$

for  $\zeta = \frac{1}{4} \min \left\{ \frac{\sqrt{c_{\min}}}{\sigma \underline{\beta}_\Theta}, \frac{\alpha_2(1-\alpha_1)}{2C\sigma \underline{\beta}_\Theta} \right\}$ . Then the optimal solution  $\hat{\theta}$  is unique with its support contained within  $S$ , and satisfies the  $\ell_\infty$ -error bound

$$\|\hat{\theta}_S - \theta_S^*\|_\infty \leq \underbrace{\frac{\sigma}{\sqrt{c_{\min}}} \left\{ \sqrt{\frac{2 \log s}{n}} + \zeta \right\}}_{B_n} + \frac{1}{\alpha_2} \lambda_n,$$

all with probability at least  $1 - 4e^{-\frac{n\zeta^2}{2}}$ . Moreover, there is no false inclusion: The solution has its support set  $\hat{S}$  contained with the true support set  $S$ .

REMARK 2. Not limited to the linear function, Lasso can also be applied to the nonlinear function class ([Plan and Vershynin 2016](#)) or nonparametric variable selection ([Li et al. 2023](#)). Moreover, there is a rich literature of representation learning that can be applied in the first stage ([Bengio et al. 2013](#)).

Theorem 5 implies that as long as  $B_n \leq \underline{\beta}_\Theta$ , the variable selection is consistent. Since  $\zeta = \frac{1}{4} \min \left\{ \frac{\sqrt{c_{\min}}}{\sigma \underline{\beta}_\Theta}, \frac{\alpha_2(1-\alpha_1)}{2C\sigma \underline{\beta}_\Theta} \right\}$ , we only need

$$\frac{\sigma}{\sqrt{c_{\min}}} \sqrt{\frac{2 \log s}{n}} + \frac{1}{\alpha_2} \cdot \frac{2C\sigma}{1 - \alpha_1} \sqrt{\frac{2 \log(d-s)}{n}} \leq \frac{1}{2} \underline{\beta}_\Theta.$$

Thus if there are  $n$  noisy samples in which

$$n \geq \max \left\{ \frac{8\sigma^2 \log s}{\underline{\beta}_\Theta^2 c_{\min}}, \frac{32C^2 \sigma^2 \log(d-s)}{(\underline{\beta}_\Theta \alpha_2 (1-\alpha_1))^2} \right\},$$



we are able to select  $s$  variables with probability at least  $1 - 4e^{-\frac{n\zeta^2}{2}}$ . Define

$$H_0(\delta, \varepsilon; \underline{\beta}_\Theta) = \max \left\{ \frac{8\sigma^2 \log s}{\underline{\beta}_\Theta^2 c_{\min}}, \frac{32C^2\sigma^2 \log(d-s)}{(\underline{\beta}_\Theta \alpha_2(1-\alpha_1))^2}, \frac{2\log(4/\delta)}{\zeta^2} \right\} = O(\sigma^2 \log d / \underline{\beta}_\Theta^2).$$

Then, when having more than  $H_0(\delta, \varepsilon; \underline{\beta}_\Theta)$  noisy labeled data at hand, we can have the correct feature selection with probability at least  $1 - \delta$ . Moreover, if we want to do one more step of refinement to restrict the uncertainty set to be within  $\mathbf{r}$ -distance where  $\mathbf{r} < \underline{\beta}_\Theta$ , then we need  $H_0(\delta, \varepsilon; \mathbf{r})$  noisy labeled data. Note that  $\mathbf{r}$ , which represents the feasible range for refinement, is the parameter that we can choose. The trade-off exists. A smaller value of  $\mathbf{r}$  demands more noisy labels in the initial stage. However, limiting the feasible region to a smaller area could conserve samples required for human comparisons. As previously noted, when both options significantly deviate from the true model, distinguishing the superior one becomes challenging. This challenge implies a greater need for samples to ascertain the correct answer. Consequently, in certain scenarios, opting for  $\mathbf{r} \leq \underline{\beta}_\Theta$  to confine the refinement region may be more optimal. Specifically, we select  $\mathbf{r}$  to minimize the total sample complexity:

$$\mathbf{r}^* = \min_{0 < \mathbf{r} \leq \underline{\beta}_\Theta} H_0(\delta, \varepsilon; \mathbf{r}) + H(\delta, \varepsilon; \mathbf{r}), \quad (4.1)$$

where  $H(\delta, \varepsilon; \mathbf{r})$  is defined in Theorem 4. It is important to emphasize that while the first part depends on the noise  $\sigma$ , the second part does not rely on  $\sigma$  but rather on the detection accuracy  $\phi(\tilde{p}(\theta))$ . Hence, the optimal  $\mathbf{r}^*$  is contingent on the function of detection accuracy. For  $\theta$  considerably distant from the true parameter  $\theta^*$ ,  $\tilde{p}(\theta)$  could potentially approach  $1/2$ , leading to a substantial value for  $\phi(\tilde{p}(\theta))$ .

### 4.3. Complexity of SFT+HC

The optimal value of  $\mathbf{r}^*$  can be obtained numerically by enumerating and comparing the objectives in Equation (4.1). To establish an upper bound on the sample complexity of the two-stage framework to analytically show the benefit, we set  $\mathbf{r} = \underline{\beta}_\Theta$ . In this case, we have

$$H_0(\delta, \varepsilon; \underline{\beta}_\Theta) = \tilde{O}(\sigma^2 / \underline{\beta}_\Theta^2) \quad \text{and} \quad H(\delta, \varepsilon; \underline{\beta}_\Theta) = \tilde{O} \left( s \bar{\phi}(a, \underline{\beta}_\Theta) + s^{1+\frac{2\kappa}{p}} / \varepsilon^{2\kappa} \right),$$

where  $\bar{\phi}(a, D) = \max_{a \leq \|\theta - \theta^*\| \leq \underline{\beta}_\Theta} \phi(\tilde{p}(\theta))$ . Theorem 6 is a direct conclusion from Theorem 4 and 5.

**THEOREM 6 (Computational complexity of SFT+HC).** *Under Assumption 4 and 5, by setting  $N_1^{HAI}(\delta) = H_0(\delta, \varepsilon; \underline{\beta}_\Theta)$  and then running Algorithm 2 with parameter range  $[-\underline{\beta}_\Theta, \underline{\beta}_\Theta]$ , it holds that  $\|\hat{\theta} - \theta^*\|_p \leq \varepsilon$  with probability at least  $1 - 2\delta$ . Moreover, under Assumption 3, the expected sample complexity is*

$$N_1^{HAI}(\delta, \varepsilon) + N_2^{HAI}(\delta, \varepsilon) = \tilde{O}(\sigma^2 / \underline{\beta}_\Theta^2 + s \bar{\phi}(a, \underline{\beta}_\Theta) + s^{1+\frac{2\kappa}{p}} / \varepsilon^{2\kappa}).$$

Theorem 6 demonstrates the sample complexity of the two-stage framework SFT+HC. When the distance is measured in two-norm (i.e.,  $p = 2$ ), the complexity is in the order of  $\tilde{O}(\sigma^2/\beta_\Theta^2 + s\bar{\phi}(a, \beta_\Theta) + s^{1+\kappa}/\varepsilon^{2\kappa})$ . Instead, if exclusively utilizing Lasso for the supervised learning oracle to refine the estimator based on  $n$  noisy labeled data, subject to certain regularity conditions, the estimation error can be bounded as  $\|\hat{\theta}_n - \theta^*\|_2 \leq c\sigma\sqrt{s\log d/n}$  with high probability for some constant  $c > 0$ . Equivalently, to ensure that the two-norm distance of the estimation error is within  $\varepsilon$ , we need to acquire  $\tilde{O}(\sigma^2 s \log d/\varepsilon^2)$  data points.

Comparing the sample complexity of SFT+HC characterized by Theorem 6 for  $p = 2$ , the condition for SFT+HC requiring less sample complexity than SFT is characterized in Proposition 4.

PROPOSITION 4. *For sufficiently small  $\varepsilon$ , SFT+HC requires less sample complexity than pure SFT for solving the  $(\varepsilon, \delta)$ -alignment problem when (ignoring the logarithm term)*

$$\frac{\sigma^2}{s^\kappa} \gtrsim \varepsilon^{2-2\kappa}. \quad (4.2)$$

We call the ratio  $\sigma^2/s^\kappa$  as *label noise-to-comparison-accuracy ratio* (LNCA ratio) and condition (4.2) as *LNCA condition*. This condition involves two important parameters: the observational noise  $\sigma$  and the convergence rate of the accuracy  $\kappa$ . When the comparison accuracy is bounded away from  $1/2$ , we have  $\kappa = 0$  and the condition reduces to  $\sigma \gtrsim \varepsilon$ , which holds naturally true. In the worst case where  $\kappa = 1$ , the condition becomes  $\sigma^2 \gtrsim s$ . When sample observational noise is higher, the benefit of the extra human comparison step becomes more apparent.

## 5. Practical Implementations

In the preceding sections, we established a framework that assumes humans can compare any two parametric models. However, such a comparison could be possibly challenging when humans only have access to the models themselves. In practice, it is often more feasible to compare models based on their performance with sampled data, allowing humans to discern which one aligns better with the true underlying model. To address this specific challenge, this section delves into the practical aspects of comparing two models using selected samples.

### 5.1. Active Learning: How to Select Samples for Comparison

Active learning focuses on the strategic selection of samples to be labeled or compared in our context, with the aim of constructing prediction models in a resource-efficient manner. The key idea is to assess the significance of a sample to determine the value of acquiring its labels. Algorithm 2 actively selects a pair of two models to ask for comparison. In practical scenarios, it often involves soliciting human judgment to compare the responses predicted by two different models for a given sample data, rather than directly comparing their model parameters.

We start with an example. The clinician needs to evaluate the Atherosclerotic Cardiovascular Disease (ASCVD) risk of patients  $f_{\theta}$ , which is a linear function of contextual information, denoted as  $x$ , such as demographics (age, gender, racial/ethnic group, and education level), baseline conditions (body mass index, history of ASCVD events, and smoking status), clinical variables (glycosylated hemoglobin (A1c) and systolic blood pressure (sbp)), anti-hypertensive agents, anti-hyperglycemic agents.

Given sample of patient context  $x \in \mathcal{X}$ , the clinician evaluates the ASCVD risk according to their expertise. The distance between model  $f_{\theta}$  and  $f_{\theta^*}$  evaluated on sample  $x$  can be defined as the absolute value of the difference:

$$d_x(\theta, \theta^*) = |\varphi(x)^\top \theta - \varphi(x)^\top \theta^*|.$$

Then the utility of  $f_{\theta}$  on sample  $x$  is  $u_x(\theta) = -d(\theta, \theta^* | x) = -|\varphi(x)^\top \theta - \varphi(x)^\top \theta^*|$ . When presented with risk levels predicted by  $f_{\theta_1}$  and  $f_{\theta_2}$ , the clinician would typically opt for the one that is closer to their assessment.

Let us first consider a simple scenario. When  $\mathcal{X}$  contains adequate variety of samples such that for any base vector  $e_i$ , there exists sample  $x$  such that  $\varphi(x) = e_i$ , then by comparing  $f_{\theta_1}$  with  $f_{\theta_2}$  on such sample  $x$ , we have

$$d_x(\theta_1, \theta^*) = |\theta_{1i} - \theta_i^*| \quad \text{and} \quad d_x(\theta_2, \theta^*) = |\theta_{2i} - \theta_i^*|.$$

It implies that the comparison of  $\theta_1$  and  $\theta_2$  when testing on  $x$  would be solely on the  $i^{\text{th}}$  dimension. Thus, the alignment process for the parameter in different dimensions can be decoupled, and SFT+HC can be directly applied where the Stage 2 alignment is proceeded along each dimension.

However, in practice, the dataset  $\mathcal{X}$  may be limited, potentially leading to situations where there are no samples  $x \in \mathcal{X}$  that satisfy the condition  $\varphi(x) = e_i$ . In such cases, it becomes impractical to refine the model parameter along each dimension separately. The question then arises: how can we efficiently select samples to refine the model parameter? To address this challenge, we propose a procedure for constructing a new basis using the available samples in  $\mathcal{X}$ . This procedure aims to optimize the alignment process by leveraging the existing data to guide the selection of samples for parameter enhancement.

## 5.2. New Basis Construction through Gram Schmidt Process

To facilitate the independent alignment of each coordinate, we aim to identify a new set of orthogonal basis, which can be constructed using  $\Psi := \{\varphi(x) : x \in \mathcal{X}\}$ . Let  $\alpha_1, \dots, \alpha_s$  represent these new basis, and our objective is to learn  $\theta^* = \sum_{i=1}^s \omega_i^* \alpha_i$ , where  $\omega_i^*$  are the corresponding coefficients. We describe the process of constructing the orthogonal basis  $\{\alpha_1, \dots, \alpha_s\}$  from the sample space.

First, we pick a set of samples that spans the space of  $\Psi$ , denoted as  $\varphi(x_1), \dots, \varphi(x_s)$ . For simplicity, we define  $\mathbf{z}_i = \varphi(x_i)$ . Then we use the Gram Schmidt process to construct a set of orthogonal basis based on  $\mathbf{z}_1, \dots, \mathbf{z}_s$ :

$$\boldsymbol{\alpha}_k = \mathbf{z}_k - \sum_{j=1}^{k-1} \frac{\mathbf{z}_k^\top \boldsymbol{\alpha}_j}{\boldsymbol{\alpha}_j^\top \boldsymbol{\alpha}_j} \boldsymbol{\alpha}_j, \quad \forall 1 \leq k \leq s.$$

We sequentially align the coordinates  $\omega_1, \dots, \omega_s$ . When evaluating on sample  $x_1$ , the true value is represented by  $\varphi(x_1)^\top \boldsymbol{\theta}^* = \mathbf{z}_1^\top \boldsymbol{\theta}^* = \omega_1^* \mathbf{z}_1^\top \mathbf{z}_1$ . Utilizing a probabilistic bisection process in 2, we actively select two answers for each query. Through this iterative refinement, the final value terminates at  $y(x_1)$ , which is guaranteed to be within  $\varepsilon$ -accuracy of the true parameter  $\omega_1^*$  (with high probability). In the end, the first coordinate is refined to  $\hat{\omega}_1 = y(x_1) / (\mathbf{z}_1^\top \mathbf{z}_1)$ .

Next, the algorithm applies testing to the sample  $\mathbf{z}_2 = \varphi(x_2) = \frac{\mathbf{z}_2^\top \boldsymbol{\alpha}_1}{\boldsymbol{\alpha}_1^\top \boldsymbol{\alpha}_1} \boldsymbol{\alpha}_1 + \boldsymbol{\alpha}_2$ . Note that the true value is given by

$$\varphi(x_2)^\top \boldsymbol{\theta}^* = \mathbf{z}_2^\top \boldsymbol{\theta}^* = \mathbf{z}_2^\top \boldsymbol{\alpha}_1 \omega_1^* + \boldsymbol{\alpha}_2^\top \boldsymbol{\alpha}_2 \omega_2^*,$$

where  $\omega_1$  is refined already. Once more, employing the probabilistic bisection process, the value of  $\mathbf{z}_2^\top \boldsymbol{\theta}^*$  is iteratively refined to  $y(x_2)$ . Upon termination of the probabilistic bisection process, we obtain the aligned value of the second coordinate as

$$\hat{\omega}_2 = \frac{y(x_2) - \mathbf{z}_2^\top \boldsymbol{\alpha}_1 \hat{\omega}_1}{\boldsymbol{\alpha}_2^\top \boldsymbol{\alpha}_2}.$$

Subsequently, at the  $k^{\text{th}}$  iteration, we test on the sample  $\mathbf{z}_k = \boldsymbol{\alpha}_k + \sum_{j=1}^{k-1} \frac{\mathbf{z}_k^\top \boldsymbol{\alpha}_j}{\boldsymbol{\alpha}_j^\top \boldsymbol{\alpha}_j} \boldsymbol{\alpha}_j$  where the true value equals

$$\mathbf{z}_k^\top \boldsymbol{\theta}^* = \sum_{j=1}^{k-1} \omega_j^* \mathbf{z}_k^\top \boldsymbol{\alpha}_j + \omega_k^* \boldsymbol{\alpha}_k^\top \boldsymbol{\alpha}_k.$$

Once the value of  $\mathbf{z}_k^\top \boldsymbol{\theta}^*$  is refined to  $y(x_k)$  through 2, we are able to obtain the aligned value of the  $k^{\text{th}}$  coordinate as

$$\hat{\omega}_k = \frac{y(x_k) - \sum_{j=1}^{k-1} \hat{\omega}_j \mathbf{z}_k^\top \boldsymbol{\alpha}_j}{\boldsymbol{\alpha}_k^\top \boldsymbol{\alpha}_k}.$$

Through asking human to evaluate  $x_1, \dots, x_s$  and refining  $\omega_1, \dots, \omega_s$  in sequence, the parameter  $\boldsymbol{\theta} := \sum_{i=1}^s \hat{\omega}_i \boldsymbol{\alpha}_i$  is refined within a certain accuracy level. We include the pseudo code in Algorithm 4.

At the end, it is essential to emphasize that the set of orthogonal basis is not unique, as there may exist multiple sets. Consequently, we can conduct multiple rounds of alignment, with the option to switch basis from one round to another.

## 6. Numerical Experiment

### 6.1. Testing Sample Complexity

In the first experiment, we compare the performance of SFT+HC and pure SFT under the same sample size.

---

**Algorithm 4** ASS (Active Sample Selection)

---

- 1: **input**: available set of covariate  $\mathcal{X}$
- 2: Pick a set of samples that spans the space of  $\Psi$ :  $\varphi(x_1), \dots, \varphi(x_s)$
- 3: **for**  $k = 1, \dots, s$  **do**

$$\alpha_k = \varphi(x_k) - \sum_{j=1}^{k-1} \frac{\varphi(x_k)^\top \alpha_j}{\alpha_j^\top \alpha_j} \alpha_j$$

- 4: **end for**
  - 5: **for**  $k = 1, \dots, s$  **do**
  - 6:   Query sample  $x_k$  through 2 and get output  $y(x_k)$ ;
  - 7:   Set  $\hat{\omega}_k = \frac{y(x_k) - \sum_{j=1}^{k-1} \hat{\omega}_j \varphi(x_k)^\top \alpha_j}{\alpha_k^\top \alpha_k}$
  - 8: **end for**
- 

*Experiment setup.* Consider a high-dimensional linear regression problem where  $d = 100$  and  $s = 10$ . The first ten coordinates of the true parameter are independently drawn from the uniform distribution and the rest coordinates are zero. The observational noise is drawn from Gaussian distribution with mean zero and variance  $\sigma = \{1, 2, 5\}$ ; we choose  $\kappa \in [0, 0.95]$ . The selection precision (along each dimension) is set as  $\varepsilon = 0.1$  and the human expert level in the choice model is  $\gamma = 1$ . We conducted 50 repetitions for each experiment and calculated the average across all results.

In the first stage the two-stage framework, we use lasso and select the sample size large enough such that the estimator for the non-zero coefficient can be deviated from zero. That is, we guarantee that important features are selected with high probability. Once the algorithm SFT+HC stops, we use the same sample size to train lasso and compute the estimation error. We compare the estimation error of two algorithms under the same sample size.

**6.1.1. Experiment results.** Figure 3 shows the ratio of the estimation error of two algorithms ( $\text{Err}(\text{SFT+HC})/\text{Err}(\text{SFT})$ ) with different values of  $\kappa$  when  $\sigma = 1$ . For smaller value of  $\kappa$ , human's selection accuracy is higher when  $\theta$  approaches  $\theta^*$ . In particular, when  $\kappa = 0$ , the selection accuracy is bounded away from 50%. Therefore, the task is harder when  $\kappa$  increases. It is consistent with the increasing trend of the estimation error when  $\kappa$  grows from 0 to 1. In addition, a larger value of  $\kappa$  leads to a larger sample size, so the estimation error of lasso decreases. The intersection point is around  $\kappa = 0.3$ . When  $\kappa \leq 0.3$ , SFT+HC performs better than pure SFT. In particular, when  $\kappa = 0$ , the error of two-stage framework is roughly 50% of that in SFT.

The results for noise levels with  $\sigma = 2$  and  $\sigma = 5$  are illustrated in Figures 4. Notably, the trends of the error curves exhibit similarity. The threshold, defined as the intersection point of these curves, is approximately 0.55 when  $\sigma = 2$ . However, when  $\sigma = 5$ , the two curves do not intersect, suggesting that SFT+HC consistently outperforms pure SFT.

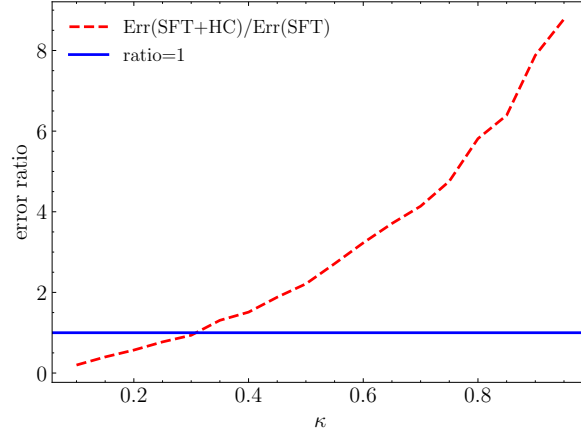
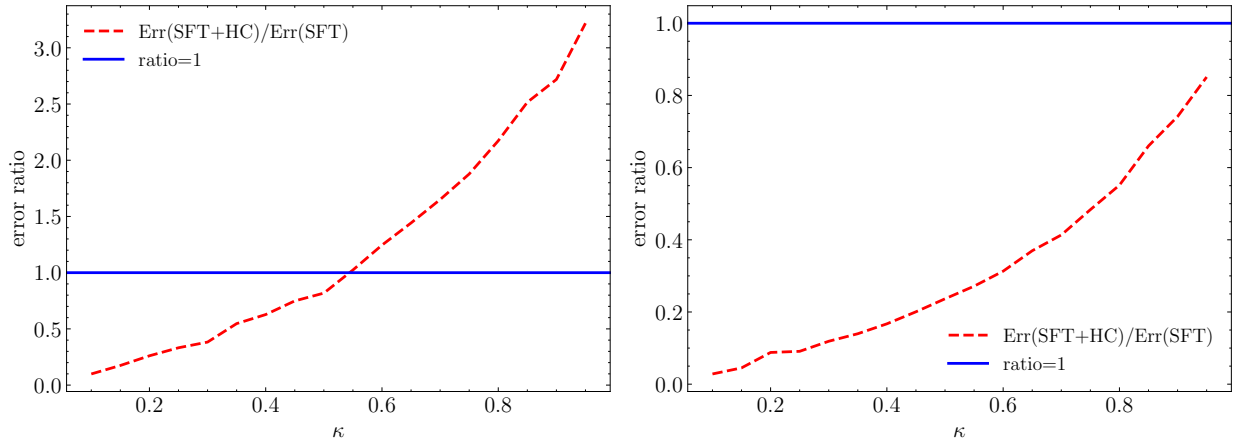


**Figure 3** Error ratio of the two-stage framework/pure SFT when  $\sigma = 1$ .

A comparison across the three figures reveals that the superiority of SFT+HC becomes more pronounced in the presence of higher observational noise. In conclusion, SFT+HC is more effective under conditions of increased noise and reduced value of  $\kappa$ .



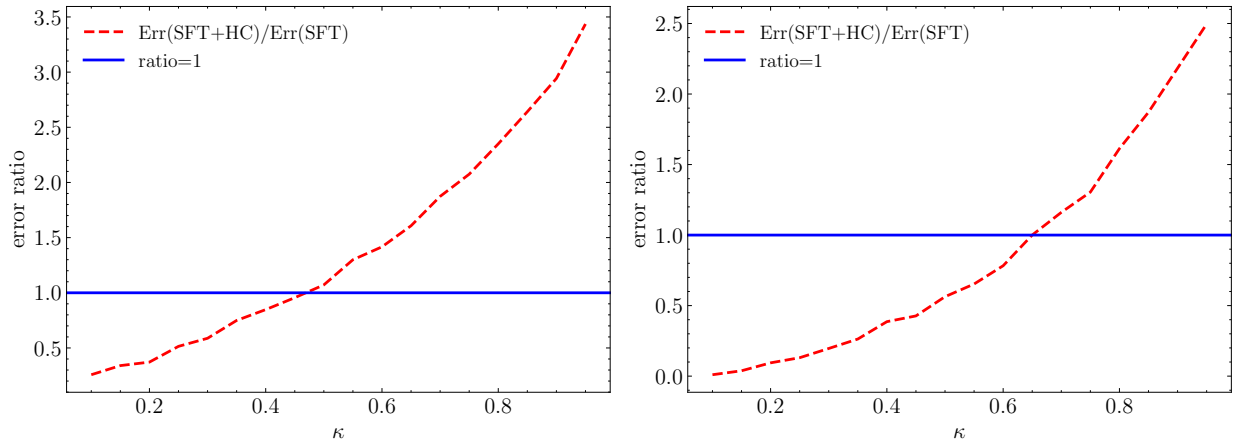
(a) Error ratio when  $\sigma = 2$ .

(b) Error ratio when  $\sigma = 5$ .

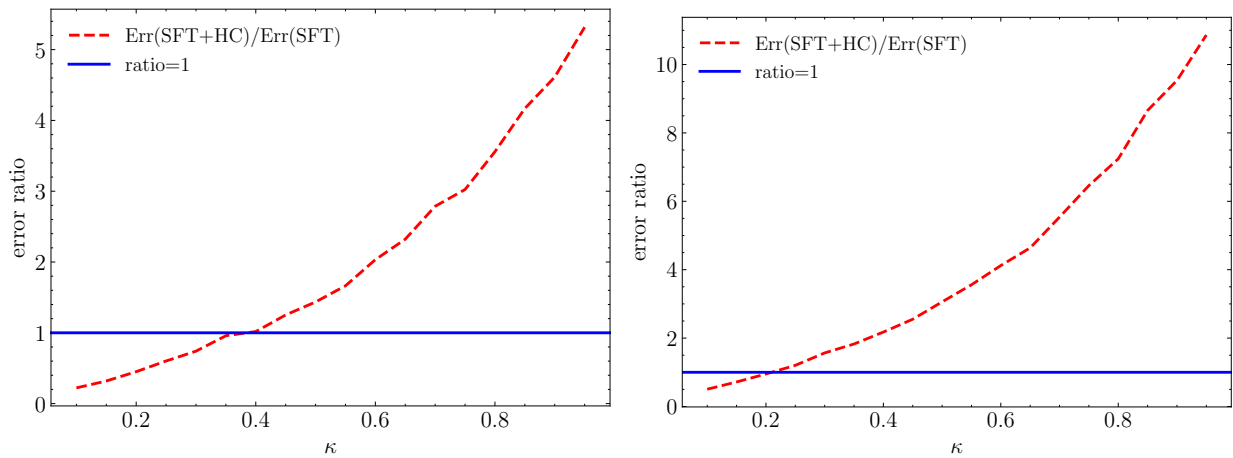
**Figure 4** Prediction errors with different noise levels.

**6.1.2. The variation of expert level  $\gamma$ .** We change the value of human expert level  $\gamma$  to see how the human comparison accuracy would influence the estimation error. The smaller value of  $\gamma$  indicates higher accuracy in the comparison task. In particular, when  $\gamma$  approaches 0, human can always select the accurate answer. Figure 5 shows the performance of two algorithms with  $\gamma = 1.1$  and  $\gamma = 0.8$ , respectively. Comparing two figures, when  $\gamma = 1.1$ , SFT+HC performs better than pure SFT when  $\kappa$  is lower than approximately 0.45; when  $\gamma = 0.8$ , SFT+HC performs better than pure SFT when  $\kappa$  is lower than approximately 0.65. Therefore, it is consistent with our theory that

SFT+HC improves its performance when human has a higher expert level in the selection (i.e., the selection accuracy is higher).

(a) Error ratio when  $\gamma = 1.1$ .(b) Error ratio when  $\gamma = 0.8$ .**Figure 5** Prediction errors with different expert levels.

**6.1.3. The variation of important feature dimensions  $s$ .** The relative performance of two algorithms also depends on the dimension of the problem. For the experiment setup, we set  $\gamma = 1$  and  $\sigma = 2$ . Figure 6 illustrates the algorithmic performance with important feature dimension  $s = 20$  and  $s = 50$ , respectively. The figure reveals that the intersection point shifts to a smaller value as the important feature dimension increases. This observation aligns with our theoretical condition (4.2), indicating that as the important feature dimension grows, the advantage of SFT+HC diminishes.

(a) Error ratio when  $s = 20$ .(b) Error ratio when  $s = 50$ .**Figure 6** Prediction errors with different important feature dimensions.



## 6.2. Testing LNCA Ratio

The LNCA ratio,  $\sigma^2/s^\kappa$ , determines the benefits of SFT+HC over pure SFT. The LNCA ratio varies between different tasks. We are interested in estimating this value for a specific task: to determine the percentage of total area enclosed by a given (red) polygon, as shown in Figure 7, for example.

We divided participants into two distinct groups. The first group was presented with the polygon figure and asked to provide their estimated percentage of the total enclosed area. The second group was shown the same figure but presented with two options for the area percentage. Their task was to select the option they believed was closer to the actual percentage of the enclosed area. For instance, in Figure 7(b), the true percentage is 50%. Human is provided with two options, 71% and 55%, so the correct choice is 55%.

This dual-group approach aimed to explore the efficacy of human estimation when directly asked to estimate the area versus when presented with comparative options. In the latter case, we varied the discrepancy between the two choices to assess how the ease or difficulty of comparison affected the accuracy of their selections. A larger disparity between the choices facilitated easier decision-making, while closer options posed a more challenging comparative task. Within Figure 7, three testing samples are depicted. Notably, sample (a) presents the most challenging comparison among these three instances due to the minimal disparity observed between them.

Fifty different tasks are launched in Amazon Mechanical Turk<sup>4</sup>, as shown in Figure 8, and we collected 1300 data points in total. We use the following ways to estimate  $\kappa$  and  $\sigma$ .

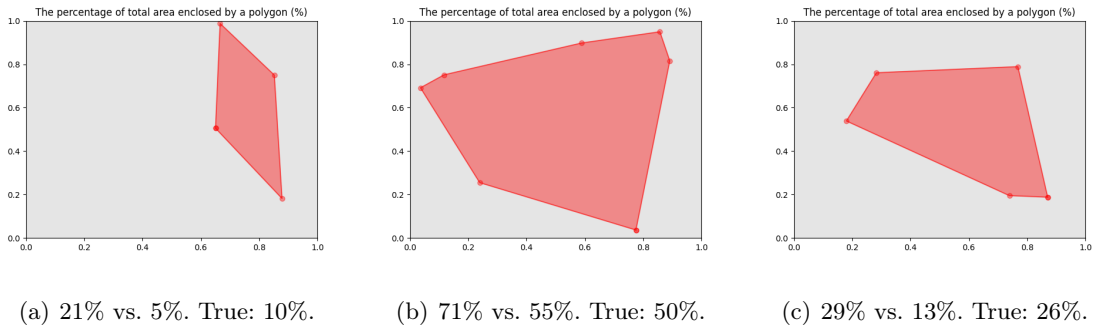
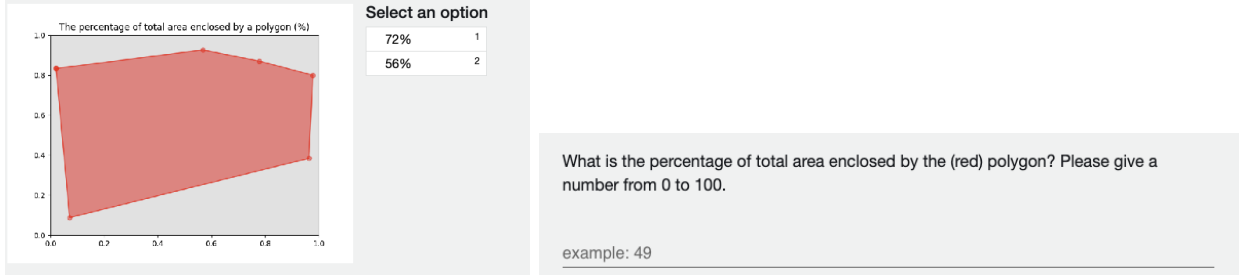


**Figure 7** Experiment design.

*Estimation process for  $\kappa$ .* Given figures with true parameter values  $\theta^*$  representing the percentage of total area enclosed by a polygon, we aim to estimate the accuracy convergence rate  $\kappa$  between two options using a human choice model. We collect multiple samples for each figure and then use these estimates to derive the relationship between the difference in utilities and the accuracy of human choices.

<sup>4</sup> <https://www.mturk.com/>



(a) The first group: Select a better answer.

(b) The second group: Estimate the percentage.

**Figure 8 Comparison vs. Estimation.**

More specifically, among two choices, assume the smaller one is  $c^-$  and the larger one is  $c^+$ , where the middle point is  $\theta = (c^- + c^+)/2$ . According to the choice model, human makes the correct choice with accuracy  $p(\theta) = \frac{1}{1 + \exp(-|u(c^-) - u(c^+)|/\gamma)}$ . Note that we try to estimate  $\kappa$  from Assumption 3 that

$$|u(c^+) - u(c^-)|/\gamma \approx \lambda_\Delta/\gamma \cdot \|\theta - \theta^*\|^\kappa.$$

That is, the accuracy is  $p(\theta) = \frac{1}{1 + \exp(-\tilde{\lambda}|\theta - \theta^*|^\kappa)}$ . Let  $\tilde{\lambda} = -\lambda_\Delta/\gamma$ . For each data point with tested point  $\theta_i$  and true parameter  $\theta_i^*$ , we define  $y_i = 1$  (the correct choice) with probability  $p_i(\theta)$  and  $y_i = 0$  (the wrong choice) with probability  $1 - p_i(\theta)$ . By maximizing the log-likelihood, we solve the optimization problem

$$\max_{\tilde{\lambda}, \kappa} \sum_{i=1}^K y_i \log p_i + (1 - y_i) \log(1 - p_i)$$

which is equivalent to

$$\max \sum_{i=1}^K -y_i \log(1 + \exp(-\tilde{\lambda}|\theta_i - \theta^*|^\kappa)) - (1 - y_i) \log(1 + \exp(\tilde{\lambda}|\theta_i - \theta_i^*|^\kappa)).$$

From the data collected from Amazon Mechanical Turk, the estimated  $\kappa$  is 0.095.

*Estimation process for  $\sigma$ .* The other group is asked to directly estimate the percentage of total area. For the figure with true parameter values  $\theta_i^*$ , human provides responses by  $y_i = \theta_i^* + \epsilon_i$ . We estimate the variance of the noise by  $\hat{\sigma}^2 = \sum_{i=1}^N \frac{(y_i - \theta_i^*)^2}{N-1} = 29.04$ .

In the context of a one-dimensional problem, as evidenced by numerical experiments detailed in the preceding section, SFT+FTPB demonstrates a substantial performance advantage over SFT when  $\kappa \approx 0.1$  and  $\sigma \approx 30$ .

## 7. Concluding Remarks

This work is motivated by the ever-growing observations of human-AI interaction in LLM. We presented a theoretical two-stage framework for explaining the significance of using human comparisons for the model improvement. While the noisy-labeled data is fed into the SFT procedure to learn the low-dimensional representation in the first stage, we sequentially inquire human evaluators to

make pair-wise comparisons in the second stage. To address the challenge of efficient acquisition of valuable information from these human comparisons, we introduced a probabilistic bisection method, which factors in the uncertainty arising from the accuracy of human comparisons. The newly introduced concept, label-noise-to-comparison-accuracy ratio, quantifies the relative scale between label noise and human comparison accuracy. We demonstrate the significant advantages of our proposed two-stage framework over pure supervised learning approach under certain conditions.

Our work represents an early attempt to organically integrate machine learning with human knowledge. We consider this paper as a prompt for an open discussion. Some potential extensions to our work are worth investigating. Firstly, we extended the probabilistic bisection algorithm from one dimension to multiple dimensions by refining along each dimension. This expansion raises the question of whether a more efficient bisection algorithm exists in multi-dimensional spaces. As discussed in [Frazier et al. \(2019\)](#), the development of a PBA tailored for multi-dimensional problems remains an open problem. Secondly, although our paper focuses on a prediction problem, the framework has the potential to be extended to the action-based learning, where the goal is to select optimal actions for the decision-making problem. Thirdly, exploring the optimal sample selection to maximize the learning algorithm's efficiency is a compelling area of inquiry. While we have outlined guidelines for practical sample selection, the quest for the most efficient proposed procedure remains open.

## References

- Akrami H, Joshi AA, Li J, Aydore S, Leahy RM (2019) Robust variational autoencoder. *arXiv preprint arXiv:1905.09961* .
- Bai Y, Jones A, Ndousse K, Askell A, Chen A, DasSarma N, Drain D, Fort S, Ganguli D, Henighan T, et al. (2022) Training a helpful and harmless assistant with reinforcement learning from human feedback. *arXiv preprint arXiv:2204.05862* .
- Balakrishnan M, Ferreira K, Tong J (2022) Improving human-algorithm collaboration: Causes and mitigation of over-and under-adherence. *Available at SSRN 4298669* .
- Balcan MF, Beygelzimer A, Langford J (2006) Agnostic active learning. *Proceedings of the 23rd international conference on Machine learning*, 65–72.
- Bastani H, Bastani O, Sinchaisri WP (2021) Improving human decision-making with machine learning. *arXiv preprint arXiv:2108.08454* .
- Bengio Y, Courville A, Vincent P (2013) Representation learning: A review and new perspectives. *IEEE transactions on pattern analysis and machine intelligence* 35(8):1798–1828.
- Benjaafar S, Wang Z, Yang X (2022) Human in the loop automation: Ride-hailing with remote (tele-) drivers. *Available at SSRN 4130757* .

- 
- Beygelzimer A, Dasgupta S, Langford J (2009) Importance weighted active learning. *Proceedings of the 26th annual international conference on machine learning*, 49–56.
- Castro R, Nowak R (2008) Active learning and sampling. *Foundations and Applications of Sensor Management*, 177–200 (Springer).
- Christiano PF, Leike J, Brown T, Martic M, Legg S, Amodei D (2017) Deep reinforcement learning from human preferences. *Advances in neural information processing systems* 30.
- Cohn D, Atlas L, Ladner R (1994) Improving generalization with active learning. *Machine learning* 15:201–221.
- D’Amour A, Heller K, Moldovan D, Adlam B, Alipanahi B, Beutel A, Chen C, Deaton J, Eisenstein J, Hoffman MD, et al. (2022) Underspecification presents challenges for credibility in modern machine learning. *The Journal of Machine Learning Research* 23(1):10237–10297.
- Deng C, Ji X, Rainey C, Zhang J, Lu W (2020) Integrating machine learning with human knowledge. *Iscience* 23(11).
- Dietvorst BJ, Simmons JP, Massey C (2015) Algorithm aversion: people erroneously avoid algorithms after seeing them err. *Journal of Experimental Psychology: General* 144(1):114.
- Dietvorst BJ, Simmons JP, Massey C (2018) Overcoming algorithm aversion: People will use imperfect algorithms if they can (even slightly) modify them. *Management science* 64(3):1155–1170.
- Dwaracherla V, Asghari SM, Hao B, Van Roy B (2024) Efficient exploration for llms. *arXiv preprint arXiv:2402.00396* .
- Frazier PI, Henderson SG, Waeber R (2019) Probabilistic bisection converges almost as quickly as stochastic approximation. *Mathematics of Operations Research* 44(2):651–667.
- Glaese A, McAleese N, Trębacz M, Aslanides J, Firoiu V, Ewalds T, Rauh M, Weidinger L, Chadwick M, Thacker P, et al. (2022) Improving alignment of dialogue agents via targeted human judgements. *arXiv preprint arXiv:2209.14375* .
- Golubev G, Levit B (2003) Sequential recovery of analytic periodic edges in binary image models. *Mathematical Methods of Statistics* 12(1):95–115.
- Hanneke S (2007) A bound on the label complexity of agnostic active learning. *Proceedings of the 24th international conference on Machine learning*, 353–360.
- Hanneke S (2011) Rates of convergence in active learning. *The Annals of Statistics* 333–361.
- Horstein M (1963) Sequential transmission using noiseless feedback. *IEEE Transactions on Information Theory* 9(3):136–143.
- Ibarz B, Leike J, Pohlen T, Irving G, Legg S, Amodei D (2018) Reward learning from human preferences and demonstrations in atari. *Advances in neural information processing systems* 31.
- Ibrahim R, Kim SH, Tong J (2021) Eliciting human judgment for prediction algorithms. *Management Science* 67(4):2314–2325.

- 
- Jaques N, Ghandeharioun A, Shen JH, Ferguson C, Lapedriza A, Jones N, Gu S, Picard R (2019) Way off-policy batch deep reinforcement learning of implicit human preferences in dialog. *arXiv preprint arXiv:1907.00456* .
- Lai TL (1977) Power-one tests based on sample sums. *The Annals of Statistics* 5(5):866–880.
- Li J, Miller AH, Chopra S, Ranzato M, Weston J (2016) Dialogue learning with human-in-the-loop. *arXiv preprint arXiv:1611.09823* .
- Li J, Xiong C, Hoi SC (2021) Learning from noisy data with robust representation learning. *Proceedings of the IEEE/CVF International Conference on Computer Vision*, 9485–9494.
- Li W, Chen N, Hong LJ (2023) Dimension reduction in contextual online learning via nonparametric variable selection. *Journal of Machine Learning Research* 24(136):1–84.
- Lowe R, Noseworthy M, Serban IV, Angelard-Gontier N, Bengio Y, Pineau J (2017) Towards an automatic turing test: Learning to evaluate dialogue responses. *arXiv preprint arXiv:1708.07149* .
- Ouyang L, Wu J, Jiang X, Almeida D, Wainwright C, Mishkin P, Zhang C, Agarwal S, Slama K, Ray A, et al. (2022) Training language models to follow instructions with human feedback. *Advances in Neural Information Processing Systems* 35:27730–27744.
- Plan Y, Vershynin R (2016) The generalized lasso with non-linear observations. *IEEE Transactions on information theory* 62(3):1528–1537.
- Reverberi C, Rigon T, Solari A, Hassan C, Cherubini P, Cherubini A (2022) Experimental evidence of effective human–ai collaboration in medical decision-making. *Scientific reports* 12(1):14952.
- Robbins H (1970) Statistical methods related to the law of the iterated logarithm. *The Annals of Mathematical Statistics* 41(5):1397–1409.
- Robbins H, Siegmund D (1974) The expected sample size of some tests of power one. *The Annals of Statistics* 2(3):415–436.
- Rodriguez S, Ludkovski M (2015) Information directed sampling for stochastic root finding. *2015 Winter Simulation Conference (WSC)*, 3142–3143 (IEEE).
- Settles B (2009) Active learning literature survey .
- Stiennon N, Ouyang L, Wu J, Ziegler D, Lowe R, Voss C, Radford A, Amodei D, Christiano PF (2020) Learning to summarize with human feedback. *Advances in Neural Information Processing Systems* 33:3008–3021.
- Sugiyama M, Nakajima S (2009) Pool-based active learning in approximate linear regression. *Machine Learning* 75:249–274.
- Sznitman R, Lucchi A, Frazier P, Jedynek B, Fua P (2013) An optimal policy for target localization with application to electron microscopy. *International Conference on Machine Learning*, 1–9 (PMLR).

- Taghanaki SA, Choi K, Khasahmadi AH, Goyal A (2021) Robust representation learning via perceptual similarity metrics. *International Conference on Machine Learning*, 10043–10053 (PMLR).
- Tsiligkaridis T, Sadler BM, Hero AO (2014) Collaborative 20 questions for target localization. *IEEE Transactions on Information Theory* 60(4):2233–2252.
- Tsou A, Vargas M, Engel A, Chiang T (2023) Foundation model’s embedded representations may detect distribution shift. *arXiv preprint arXiv:2310.13836* .
- Wainwright MJ (2019) *High-dimensional statistics: A non-asymptotic viewpoint*, volume 48 (Cambridge university press).
- Wu X, Xiao L, Sun Y, Zhang J, Ma T, He L (2022) A survey of human-in-the-loop for machine learning. *Future Generation Computer Systems* 135:364–381.
- Xu W, Dong S, Arumugam D, Van Roy B (2023) Shattering the agent-environment interface for fine-tuning inclusive language models. *arXiv preprint arXiv:2305.11455* .
- Zhou C, Paffenroth RC (2017) Anomaly detection with robust deep autoencoders. *Proceedings of the 23rd ACM SIGKDD international conference on knowledge discovery and data mining*, 665–674.
- Zhou W, Xu K (2020) Learning to compare for better training and evaluation of open domain natural language generation models. *Proceedings of the AAAI Conference on Artificial Intelligence*, volume 34, 9717–9724.
- Zhu B, Jiao J, Jordan MI (2023) Principled reinforcement learning with human feedback from pairwise or  $k$ -wise comparisons. *arXiv preprint arXiv:2301.11270* .
- Ziegler DM, Stiennon N, Wu J, Brown TB, Radford A, Amodei D, Christiano P, Irving G (2019) Fine-tuning language models from human preferences. *arXiv preprint arXiv:1909.08593* .

## Appendix A: Proofs

### A.1. Proofs in Section 3

*Proof of Lemma 1.* Without loss of generality, assume  $d(\boldsymbol{\theta}_1, \boldsymbol{\theta}^*) < d(\boldsymbol{\theta}_2, \boldsymbol{\theta}^*)$ . Then the probability that human will make the right selection (i.e., select  $f_{\boldsymbol{\theta}_1}$ ), is

$$\begin{aligned} \mathbb{P}(f_{\boldsymbol{\theta}_1} \succeq f_{\boldsymbol{\theta}_2}) &= \mathbb{P}(U(\boldsymbol{\theta}_1) > U(\boldsymbol{\theta}_2)) \\ &= \frac{\exp(u(\boldsymbol{\theta}_1)/\gamma)}{\exp(u(\boldsymbol{\theta}_1)/\gamma) + \exp(u(\boldsymbol{\theta}_2)/\gamma)} = \frac{1}{1 + \exp((u(\boldsymbol{\theta}_2) - u(\boldsymbol{\theta}_1))/\gamma)}. \end{aligned}$$

Since  $u(\boldsymbol{\theta}_2) < u(\boldsymbol{\theta}_1)$ , we can similarly prove the conclusion when  $d(\boldsymbol{\theta}_1, \boldsymbol{\theta}^*) > d(\boldsymbol{\theta}_2, \boldsymbol{\theta}^*)$ .  $\square$

*Proof of Proposition 1.* At each round, the algorithm filters a half of the space. Therefore, when the total number of round  $k$  satisfies that

$$\frac{2\beta_{\Theta}}{2^k} \leq \varepsilon,$$

we are able to reach the conclusion that  $|\theta_k - \theta^*| \leq \varepsilon$ . The condition is equivalent to

$$k \geq \log_2 \left( \frac{\beta_{\Theta}}{\varepsilon} \right) + 1.$$

$\square$

*Proof of Lemma 2.* We first show that for a chosen confidence parameter  $\eta \in (0, 1)$  and  $\tilde{h}_m = (2m(\ln(m+1) - \ln \eta))^{1/2}$ , such a test satisfies  $\mathbb{P}(\tau_1^\dagger(\theta) < \infty) \leq \eta$  if  $\theta = \theta^*$ . Note that  $S_m(\theta) = \sum_{i=1}^m \tilde{Z}_i(\theta)$  and  $\mathbb{P}(\tilde{Z}_i(\theta) = 1) = \tilde{p}(\theta)$ .

Define  $Q_m = \sum_{i=1}^m X_i$ , where  $X_i$  are i.i.d. Bernoulli random variables with  $\mathbb{P}(X_i = 1) = p = 1 - \mathbb{P}(X_i = 0)$ . Robbins (1970) has shown that  $\mathbb{P}(\tau' < \infty) \leq \eta$ , where

$$\tau' = \inf \left\{ m \geq 1 : \binom{m}{Q_m} p^{Q_m} (1-p)^{m-Q_m} \leq \eta / (m+1) \right\}.$$

This test stops at some  $m$  if  $Q_m = \tilde{h}$  such that  $\mathbb{P}(Q_m = \tilde{h}) \leq \eta / (m+1)$ . Define the other stopping time:

$$\tau'' = \inf \{ m \geq 1 : |Q_m - m\tilde{p}| \geq (m(\ln(m+1) - \ln \eta)/2)^{1/2} \}.$$

We will show that  $\mathbb{P}(\tau'' < \infty) \leq \mathbb{P}(\tau' < \infty) \leq \eta$ . For  $\tilde{h} \geq m\tilde{p} + (m(\ln(m+1) - \ln \eta)/2)^{1/2}$ , Hoeffding's inequality yields

$$\mathbb{P}(Q_m = \tilde{h}) \leq \mathbb{P}(Q_m \geq \tilde{h}) \leq \exp(-2m(\tilde{h}/m - \tilde{p})^2) \leq \eta / (m+1).$$

Similarly, for  $\tilde{h} \leq m\tilde{p} - (2m(\ln(m+1) - \ln \eta))^{1/2}$ , Hoeffding's inequality yields

$$\mathbb{P}(Q_m = \tilde{h}) \leq \mathbb{P}(Q_m \leq \tilde{h}) \leq \exp(-2m(\tilde{h}/m - \tilde{p})^2) \leq \eta / (m+1).$$

Since  $\mathbb{P}(Q_m = \tilde{h}) \leq \eta / (m+1)$  for any  $\tilde{h} \geq m\tilde{p} + (m(\ln(m+1) - \ln \eta)/2)^{1/2}$  or  $\tilde{h} \leq m\tilde{p} - (2m(\ln(m+1) - \ln \eta))^{1/2}$ , we have  $\tau'' \geq \tau'$ , which implies that

$$\mathbb{P}(\tau'' < \infty) \leq \mathbb{P}(\tau' < \infty) \leq \eta.$$

Since  $\tilde{p}(\theta^*) = 1/2$  and  $S_m(\theta^*) = 2(Q_m - mp)$  with  $p = 1/2$ , then by setting  $\tilde{h}_m = (2m(\ln(m+1) - \ln \eta))^{1/2}$ , we have

$$\begin{aligned} \tau'' &= \inf \{ m \geq 1 : |Q_m - m\tilde{p}| \geq (m(\ln(m+1) - \ln \eta)/2)^{1/2} \} \\ &= \inf \{ m \geq 1 : |S_m(\theta^*)| \geq (2m(\ln(m+1) - \ln \eta))^{1/2} \} \\ &= \inf \{ m \geq 1 : |S_m(\theta^*)| \geq \tilde{h}_m \}. \end{aligned}$$



According to the definition, we have

$$\mathbb{P}(\tau_1^\uparrow(\theta^*) < \infty) \leq \eta.$$

Let  $S(0)$  denote the zero-drift random walk. On the event  $\theta_k > \theta^*$ ,

$$\mathbb{P}(Z_k(\theta_k) = +1 | \theta_k) = \mathbb{P}(S_{k, \tau_1^\uparrow(\theta_k)} > 0, \tau_1^\uparrow(\theta_k) < \infty | \theta_k) \leq \mathbb{P}(S_{\tau_1^\uparrow(\theta^*)} > 0, \tau_1^\uparrow(\theta^*) < \infty) \leq \eta/2,$$

where the first inequality follows by a sample path argument and the second inequality by the property that  $\mathbb{P}(\tau_1^\uparrow(\theta^*) < \infty) \leq \eta$ . Similarly, it can be shown that on the event  $\theta_k < \theta^*$ ,

$$\mathbb{P}(Z_k(\theta_k) = -1 | \theta_k) \leq \eta/2.$$

We use  $p(\theta)$  to denote the the probability of correctness when the testing stops.<sup>5</sup> Therefore, for  $\theta \in \Theta \setminus \{\theta^*\}$ , we have accuracy  $p(\theta) \geq 1 - \eta/2 > 1/2$ , where  $p(\theta) = \mathbb{P}(Z_k(\theta) = +1)$  if  $\theta < \theta^*$  and  $p(\theta) = \mathbb{P}(Z_k(\theta) = -1)$  if  $\theta > \theta^*$ . Define  $p_c = 1 - \eta/2$  as the comparison accuracy, which can be chosen by the algorithm through the selection of  $\eta$ .  $\square$

*Proof of Lemma 3.* Let  $U_0 = \tau(a)$ . Lemma 3 in [Frazier et al. \(2019\)](#) establishes that  $U_0$  is finite a.s. Now, for  $j \geq 1$ , we recursively define

$$V_j = \inf\{i > U_{j-1} : \nu_i(A) \geq 1/2\}, \text{ and } U_j = \inf\{i > V_j : \nu_i(B) \geq 1 - \Delta\}.$$

Here,  $V_j$  represents the first time after time  $U_{j-1}$  that the conditional mass in  $A$  becomes at least  $1/2$ , and  $U_j$  is the first time after  $V_j$  that the conditional mass in  $B$  is once again at least  $1 - \Delta$ .  $U_j$  and  $V_j$  for  $j \geq 1$  taking the value  $\infty$  implicitly implies that the corresponding event does not occur. Let  $\Gamma$  be the number of ‘‘cycles’’, i.e.,  $\Gamma = \sum_{j=1}^{\infty} \mathbf{1}(V_j < \infty)$ . It holds that

$$T(a) = U_0 + \sum_{j=1}^{\Gamma} [(V_j - U_{j-1}) + (U_j - V_j)]. \quad (\text{A.1})$$

In the above expression,  $V_j - U_{j-1}$  represents the  $j^{\text{th}}$  time required to increase the conditional mass in  $A$  from below  $\Delta$  to  $1/2$  or more. The quantity  $U_j - V_j$  (conditional on  $\Gamma \geq j$ , i.e., conditional on both  $U_j$  and  $V_j$  being finite), represents the number of steps required to return the conditional mass to at least  $1 - \Delta$ , starting from a point where the conditional mass in  $A$  is at least  $1/2$ .

Using Equation (A.1), it can be shown that (Equation (6) in [Frazier et al. \(2019\)](#))

$$T(a) \leq_{s.t.} \tau(a) + R, \quad (\text{A.2})$$

where  $R$  is a random variable that is independent of  $\tau(a)$  and  $a$ .  $\square$

*Proof of Lemma 4.* For ease of notation, let  $\tau = \tau(a) = \inf\{k \geq 0 : \nu_k(B) > 1 - \Delta, \theta_k < \theta^*\}$ . Recall that  $\nu_k(D) = \mu_k(D \cap [-\beta_\Theta, \theta^*]) / \mu_k([-\beta_\Theta, \theta^*])$ .

Fix  $\iota \in (0, 1/2)$ . Define

$$M_k = e^{r_2 \tilde{N}(k \wedge \tau)} / \nu_{k \wedge \tau}(B),$$

<sup>5</sup> Note that  $\tilde{p}(\theta)$  denotes the probability of accuracy from one sample while  $p(\theta)$  denotes the probability of accuracy when the testing stops (based on multiple samples).

where

$$\tilde{N}(k) = \sum_{j=1}^{k-1} \mathbf{1}(\mu_j([- \beta_{\Theta}, \theta^*]) \geq 1/2 + \iota)$$

is the number of instances from time 0 to time  $k-1$  when the mass of  $A \cup B$  is at least  $1/2 + \iota$ . It has been shown in Lemma 2 in [Frazier et al. \(2019\)](#) that  $\{M_k : k \geq 0\}$  is a supermartingale with respect to the filtration  $\mathcal{F}$ , for some  $r_2$  (which depends only on  $\Delta$ ,  $\eta$ ,  $p_c$ , and  $p$ ). According to the supermartingale property and the assumption that  $\mu_0(B) \geq a^\varsigma > 0$ , we have that

$$\mathbb{E}[e^{r_2 \tilde{N}(k \wedge \tau)}] \leq \mathbb{E} \left[ \frac{e^{r_2 \tilde{N}(k \wedge \tau)}}{\nu_{k \wedge \tau}(B)} \right] = \mathbb{E}[M_k] \leq \mathbb{E}[M_0] = \frac{1}{\mu_0(B)} = \frac{\theta^*}{a^\varsigma}.$$

Since  $\tilde{N}(\cdot)$  is nondecreasing, so  $e^{r_2 \tilde{N}(n \wedge \tau)} \uparrow e^{r_2 \tilde{N}(\tau)}$  as  $\tilde{N} \rightarrow \infty$ . Monotone convergence then yields

$$\mathbb{E}e^{r_2 \tilde{N}(\tau)} = \lim_{k \rightarrow \infty} \mathbb{E}[e^{r_2 \tilde{N}(k \wedge \tau)}] \leq \theta^* / a^\varsigma.$$

For  $a = \omega e^{-rk}$ , we obtain

$$\mathbb{E}[e^{r_2 \tilde{N}(\tau(\omega e^{-rk}))}] \leq \theta^* / \nu(a) \leq \theta^* / (\omega e^{-rk})^\varsigma = e^{\varsigma r k} \theta^* / \omega^\varsigma.$$

Lemma 1 in [Frazier et al. \(2019\)](#) shows that there exists some  $\alpha > 0$  such that

$$\mathbb{P}(\tilde{N}(k/2) \leq \alpha k/2) \leq \beta e^{-r_1 k/2}.$$

Hence, we can bound

$$\begin{aligned} \mathbb{P}(\tau(\omega e^{-rk}) > k/2) &\leq \mathbb{P}(\tilde{N}(\tau(\omega e^{-rk})) \geq \tilde{N}(k/2)) \\ &\leq P(\tilde{N}(\tau(\omega e^{-rk})) \geq \tilde{N}(k/2), \tilde{N}(k/2) > \alpha k/2) + \mathbb{P}(\tilde{N}(k/2) \leq \alpha k/2) \\ &\leq P(\tilde{N}(\tau(\omega e^{-rk})) > \alpha k/2) + \beta_1 e^{-r_1 k/2} \\ &\leq e^{-r_2 \alpha k/2} \mathbb{E}[e^{r_2 \tilde{N}(\tau(\omega e^{-rk}))}] + \beta_1 e^{-r_1 k/2} \\ &\leq e^{-r_2 \alpha k/2} \cdot \frac{\theta^*}{\omega^\varsigma} e^{\varsigma r k} + \beta_1 e^{-r_1 k/2} \\ &= e^{\varsigma r k - r_2 \alpha k/2} \cdot \frac{\theta^*}{\omega^\varsigma} + \beta_1 e^{-r_1 k/2}. \end{aligned}$$

By setting  $r = \frac{r_2 \alpha}{4\varsigma}$ , we have

$$\mathbb{P}(\tau(\omega e^{-rk}) > k/2) \leq e^{-r_2 \alpha k/4} \cdot \frac{\theta^*}{\omega^\varsigma} + \beta_1 e^{-r_1 k/2}.$$

□

*Proof of Theorem 1.* Lemma 3 has established that

$$T(a) \leq_{s.t.} \tau(a) + R,$$

where  $\tau(a)$  and  $R$  are independent random variables with appropriately light tails and the non-negative random variable  $R$  does not depend on  $a$ .

For arbitrary  $\omega > 0$ , we have

$$\begin{aligned} &\mathbb{P}(e^{rk} |\theta_k - \theta^*| \mathbf{1}(\theta_k \leq \theta^*) > \omega) = \mathbb{P}(\theta^* - \theta_k > \omega e^{-rk}) \\ &\leq \mathbb{P}(T(\omega e^{-rk}) > k) \leq \mathbb{P}(\tau(\omega e^{-rk}) + R > k) \\ &\leq \mathbb{P}(\tau(\omega e^{-rk}) > k/2) + \mathbb{P}(R > k/2). \end{aligned}$$

Lemma 4 establishes that

$$\mathbb{P}(\tau(\omega e^{-rk}) > k/2) \leq e^{-r_2 \alpha k/4} \cdot \frac{\theta^*}{\omega^\varsigma} + \beta_1 e^{-r_1 k/2}, \quad (\text{A.3})$$

where  $r = r_2 \alpha / (4\zeta)$ .

Moreover, Lemma 9 in Frazier et al. (2019) shows that  $R$  has an exponentially decaying tail, i.e.,

$$\mathbb{P}(R > k/2) \leq \beta_2 e^{-r_R k}, \quad (\text{A.4})$$

where  $r_R$  does not depend on  $a$ .

Fix some  $\omega > 0$  (which we will define later) and define

$$\tau^\rightarrow(\delta, \varepsilon) = \max \left\{ \frac{\log(\omega/\varepsilon)}{r}, \frac{4 \log(8\theta^*/(\delta\omega^\varsigma))}{r_2 \alpha}, \frac{2 \log(8\beta_1/\delta)}{r_1}, \frac{\log(8/\delta)}{r_R} \right\}.$$

For any  $k$  such that  $k \geq \tau^\rightarrow(\delta, \varepsilon)$ , the probability of the precision  $|\theta_k - \theta^*|$  being larger than  $\varepsilon$  can be bounded by

$$\begin{aligned} & \mathbb{P}(|\theta_k - \theta^*| > \varepsilon) \\ &= \mathbb{P}(|\theta_k - \theta^*| e^{rk} > \varepsilon e^{rk}) \\ &= \mathbb{P}(e^{rk} |\theta_k - \theta^*| > \omega) \\ &= \mathbb{P}(e^{rk} |\theta_k - \theta^*| \mathbf{1}(\theta_k \leq \theta^*) > \omega) + \mathbb{P}(e^{rk} |\theta_k - \theta^*| \mathbf{1}(\theta_k > \theta^*) > \omega) \\ &\leq 2 (\mathbb{P}(\tau(\omega e^{-rk}) > k/2) + \mathbb{P}(R > k/2)) \\ &\stackrel{(\text{A.3}), (\text{A.4})}{\leq} 2 \left( e^{-r_2 \alpha k/4} \cdot \frac{\theta^*}{\omega^\varsigma} + \beta_1 e^{-r_1 k/2} + \beta_2 e^{-r_R k} \right) \\ &\leq \delta, \end{aligned}$$

where the last inequality holds since  $k \geq \tau^\rightarrow(\delta, \varepsilon)$  implies

$$e^{-r_2 \alpha k/4} \frac{\theta^*}{\omega^\varsigma} \leq \delta/8, \quad \beta_1 e^{-r_1 k/2} \leq \delta/8, \quad \beta_2 e^{-r_R k} \leq \delta/8.$$

Specifically, we take  $\omega$  such that

$$\omega/\varepsilon = 8\theta^*/(\delta\omega^\varsigma)$$

which is equivalent to

$$\omega = \left( \frac{8\theta^* \varepsilon}{\delta} \right)^{\frac{1}{1+\varsigma}}.$$

In this case,

$$\begin{aligned} \tau^\rightarrow(\delta, \varepsilon) &= \max \left\{ \frac{4\zeta(1+\varsigma) \log(\frac{8\theta^*}{\delta\varepsilon^\varsigma})}{r_2 \alpha}, \frac{4 \log(\frac{8\theta^*}{\delta\varepsilon^\varsigma})}{r_2 \alpha}, \frac{2 \log(8\beta_1/\delta)}{r_1}, \frac{\log(8\beta_2/\delta)}{r_R} \right\} \\ &= \max \left\{ \frac{4\zeta(1+\varsigma) \log(\frac{8\theta^*}{\delta\varepsilon^\varsigma})}{r_2 \alpha}, \frac{2 \log(8\beta_1/\delta)}{r_1}, \frac{\log(8\beta_2/\delta)}{r_R} \right\}. \end{aligned}$$

□

*Proof of Proposition 2.* From the proof of Theorem 1, for any  $k$ , by substituting  $\omega = a e^{rk}$  in (A.3), we have

$$\begin{aligned} \mathbb{P}(T(a) > k) &\leq \mathbb{P}(\tau(a) + R > k) \\ &\leq \mathbb{P}(\tau(a) > k/2) + \mathbb{P}(R > k/2) \\ &\leq e^{-r_2 \alpha k/2} \cdot \frac{\theta^*}{a} + \beta_1 e^{-r_1 k/2} + \beta_2 e^{-r_R k}. \end{aligned}$$

Since

$$\mathbb{P}(\psi(a) > k) = \mathbb{P}(\max\{T(a), T'(a)\} > k) \leq \mathbb{P}(T(a) > k) + \mathbb{P}(T'(a) > k),$$

and  $\mathbb{P}(T'(a) > k) = \mathbb{P}(T(a) > k)$  because of symmetricity, we have

$$\mathbb{P}(\psi(a) > k) \leq 2(e^{-r_2 \alpha k/2} \theta^* / a + \beta_1 e^{-r_1 k/2} + \beta_2 e^{-r_R k}).$$

Taking expectation of  $\psi(a)$ ,

$$\begin{aligned} \mathbb{E}[\psi(a)] &= \int_0^\infty P(\psi(a) > s) ds \\ &\leq 2 \int_0^\infty \left( e^{-r_2 \alpha s/2} \cdot \frac{\theta^*}{a} + \beta_1 e^{-r_1 s/2} + \beta_2 e^{-r_R s} \right) ds \\ &= \frac{4\theta^*}{r_2 \alpha a} + \frac{4\beta_1}{r_1} + \frac{2\beta_2}{r_R}. \end{aligned}$$

□

*Proof of Lemma 5.* Let  $N^\dagger(q)$  denote the number of vertical tests needed when the drift is  $q$  (which equals  $2\tilde{p}(\theta) - 1$ ). From [Robbins and Siegmund \(1974\)](#) and [Lai \(1977\)](#), we have

$$\limsup_{q \rightarrow 0} \mathbb{E}[N^\dagger(q)] q^2 (\ln(|q^{-1}|))^{-1} < \infty.$$

Then, there exists  $c_1 > 0$  and  $q_0$  such that

$$\mathbb{E}[N^\dagger(q)] q^2 (\ln(|q^{-1}|))^{-1} < c_1, \quad \forall q \leq q_0.$$

Moreover,  $\mathbb{E}[N^\dagger(q)]$  is decreasing in  $q$ . It implies that there exists  $p_0$  such that

$$\begin{aligned} \mathbb{E}[\tau_1^\dagger(\theta)] &\leq c_1 |2\tilde{p}(\theta) - 1|^{-2} \ln(|2\tilde{p}(\theta) - 1|^{-1}) \mathbf{1}(|2\tilde{p}(\theta) - 1| \leq p_0) + c_2 \mathbf{1}(|2\tilde{p}(\theta) - 1| > p_0) \\ &\leq c_1 |2\tilde{p}(\theta) - 1|^{-2} \ln(|2\tilde{p}(\theta) - 1|^{-1}) + c_2. \end{aligned}$$

Thus, we have reached our conclusion. □

**LEMMA 7.** *Suppose  $\tilde{p}(\theta)$  is strictly larger than  $1/2$  for any  $\theta \neq \theta^*$ . There exists  $\delta' > 0$  such that  $\tilde{p}(\theta) > 1/2 + \delta'$  for all  $\theta \in [-\beta_\Theta, \theta^* - a] \cup [\theta^* + a, -\beta_\Theta]$ .*

*Proof of Lemma 7.* For any  $\theta \in [-\beta_\Theta, \theta^* - a] \cup [\theta^* + a, -\beta_\Theta]$ , there exists an open ball  $\mathcal{B}(\theta)$  containing  $\theta$  and  $\delta(\theta) > 0$  such that  $\tilde{p}(\theta') > 1/2 + \delta(\theta)$  for all  $\theta' \in \mathcal{B}(\theta)$ . According to Heine–Borel Theorem, there exists finite number of covers  $\mathcal{B}(\theta_1), \dots, \mathcal{B}(\theta_k)$  such that  $[-\beta_\Theta, \theta^* - a] \cup [\theta^* + a, -\beta_\Theta] \subseteq \bigcup_{i=1}^k \mathcal{B}(\theta_i)$ . Let  $\delta' = \min_{1 \leq i \leq k} \delta(\theta_i)$ . Then we conclude that  $\tilde{p}(\theta) > 1/2 + \delta'$  for all  $\theta \in [-\beta_\Theta, \theta^* - a] \cup [\theta^* + a, -\beta_\Theta]$ . □

*Proof of Proposition 3.* Define

$$\tilde{p}_{\min}(a, \mathbf{r}) = \min_{\theta: a \leq |\theta - \theta^*| \leq \mathbf{r}} \tilde{p}(\theta).$$

First, we note that  $\tau_1^\dagger(\theta)$  decreases (stochastically) in  $\theta$ . Let  $W_k$  be independent and identically distributed random variables that denotes the number of power-one tests needed when the drift is  $2\tilde{p}_{\min}(a, \mathbf{r}) - 1$ ; that is  $W_k =_D N^\dagger(2\tilde{p}_{\min}(a, \mathbf{r}) - 1)$ . Then we have

$$\tau_1^\dagger(\theta_k) \mathbf{1}(\|\theta_k - \theta^*\| \geq a) \leq_{s.t.} W_k.$$

Lemma 5 indicates

$$\mathbb{E}[W_k] \leq c_1 |2\tilde{p}_{\min}(a, \mathbf{r}) - 1|^{-2} \ln(|2\tilde{p}_{\min}(a, \mathbf{r}) - 1|^{-1}) + c_2.$$

Therefore,

$$\begin{aligned} \mathbb{E} \left[ \sum_{k=1}^{\psi(a)} T^\uparrow(\theta_k) \mathbf{1}(\|\theta_k - \theta^*\| \geq a) \right] &\leq \mathbb{E} \left[ \sum_{k=1}^{\psi(a)} W_k \right] \stackrel{(*)}{=} \mathbb{E}[\psi(a)] \mathbb{E}[W] \\ &\leq \left( \frac{4\theta^*}{r_2 \alpha a} + \frac{4\beta_1}{r_1} + \frac{2\beta_2}{r_R} \right) \max_{a \leq \|\theta - \theta^*\| \leq \beta_\Theta} \phi(\tilde{p}(\theta)), \end{aligned}$$

where we apply Wald's equation for (\*).  $\square$

*Proof of Theorem 2.* The design of the algorithm implies that the algorithm stops before  $\tau^\rightarrow(\delta, \varepsilon)$  horizontal moves, so we have

$$T^\rightarrow \leq \tau^\rightarrow(\delta, \varepsilon).$$

Let  $W_k =_D N^\uparrow(2\underline{p} - 1)$  where  $=_D$  denotes ‘‘distributionally equal’’. Then we have

$$\begin{aligned} \mathbb{E} \left[ \sum_{k=1}^{T^\rightarrow} T^\uparrow(\theta_k) \right] &\leq \mathbb{E} \left[ \sum_{k=1}^{T^\rightarrow} W_k \right] \leq \tau^\rightarrow(\delta, \varepsilon) \cdot \mathbb{E}[W] \\ &\leq \tau^\rightarrow(\delta, \varepsilon) \cdot \phi(\underline{p}), \end{aligned}$$

where the last inequality is implied by Proposition 5.  $\square$

*Proof of Lemma 6.* According to the definition,

$$\tilde{p}(\theta) = \frac{1}{1 + \exp(-|u(c_\Delta^+(\theta)) - u(c_\Delta^-(\theta))|/\gamma)}.$$

For ease of notation, define  $z = |u(c_\Delta^+(\theta)) - u(c_\Delta^-(\theta))|$ . Then the condition  $\tilde{p}(\theta) - 1/2 \geq c|\theta - \theta^*|^\kappa$  is equivalent to

$$\begin{aligned} \frac{1}{1 + \exp(-z/\gamma)} - \frac{1}{2} &\geq c|\theta - \theta^*|^\kappa \\ \Leftrightarrow z/\gamma &\geq -\ln \left( \frac{1 - 2c|\theta - \theta^*|^\kappa}{1 + 2c|\theta - \theta^*|^\kappa} \right) = -\ln \left( 1 - \frac{4c|\theta - \theta^*|^\kappa}{1 + 2c|\theta - \theta^*|^\kappa} \right). \end{aligned} \quad (\text{A.5})$$

When  $|\theta - \theta^*| \leq a$ , we can choose  $c < 1/(6a)$  such that

$$\frac{4c|\theta - \theta^*|^\kappa}{1 + 2c|\theta - \theta^*|^\kappa} < \frac{1}{2}.$$

Note that  $-\ln(1-x) \leq 2\ln(2)x$  when  $x < 1/2$ . Then substituting  $x$  with  $\frac{4c|\theta - \theta^*|^\kappa}{1 + 2c|\theta - \theta^*|^\kappa}$ , it holds that

$$-\ln \left( 1 - \frac{4c|\theta - \theta^*|^\kappa}{1 + 2c|\theta - \theta^*|^\kappa} \right) \leq 2\ln(2) \frac{4c|\theta - \theta^*|^\kappa}{1 + 2c|\theta - \theta^*|^\kappa}.$$

Therefore, to achieve the condition (A.5), we only need

$$z/\gamma \geq 8\ln(2)c|\theta - \theta^*|^\kappa \geq 2\ln(2) \frac{4c|\theta - \theta^*|^\kappa}{1 + 2c|\theta - \theta^*|^\kappa},$$

then we will have

$$z/\gamma \geq 8\ln(2)c|\theta - \theta^*|^\kappa \geq 2\ln(2) \frac{4c|\theta - \theta^*|^\kappa}{1 + 2c|\theta - \theta^*|^\kappa} \geq -\ln \left( 1 - \frac{4c|\theta - \theta^*|^\kappa}{1 + 2c|\theta - \theta^*|^\kappa} \right).$$

Thus, we only need

$$|u(c_\Delta^+(\theta)) - u(c_\Delta^-(\theta))| \geq 8\ln(2)c\gamma|\theta - \theta^*|^\kappa,$$

then the condition (A.5) holds. Under Assumption 3, we choose  $c = \min\{\lambda_\Delta/(8\gamma\ln(2)), 1/(6a)\}$  and the conclusion holds.  $\square$

*Proof of Theorem 3.* From Theorem 1, when the horizontal move  $T^\rightarrow \geq \tau_1^\rightarrow(a, \delta/2)$ , it holds with probability at least  $1 - \delta/2$  that

$$\mathbb{P}(\|\theta_{T^\rightarrow} - \theta^*\| \leq a) \geq 1 - \delta/2.$$

Define event  $\mathcal{E}_k = \{\|\theta_k - \theta^*\| \leq a\}$  and let  $\theta = \theta_{T^\rightarrow}$  for simplicity. Under event  $\mathcal{E}_{T^\rightarrow}$ , Lemma 6 implies that  $\tilde{p}(\theta) - 1/2 \geq c|\theta - \theta^*|^\kappa$  for  $c = \min\{\lambda_\Delta/(8\gamma \ln(2)), 1/(6a)\}$ . Therefore, as long as

$$\tilde{p}(\theta) - 1/2 \leq c\varepsilon^\kappa,$$

we have that  $|\theta - \theta^*| \leq \varepsilon$ . Recall that

$$\tilde{p}(\theta') = \begin{cases} \mathbb{P}(\tilde{Z}(\theta') = 1), & \text{if } \theta' \leq \theta^* \\ \mathbb{P}(\tilde{Z}(\theta') = -1), & \text{if } \theta' > \theta^* \end{cases}.$$

WLOG, assume  $\theta < \theta^*$ . According to Hoeffding's inequality, for any  $s > 0$  and  $n > 0$ , we have

$$\mathbb{P}\left(\left|\sum_{i=1}^n \tilde{Z}_i(\theta)/n - (2\tilde{p}(\theta) - 1)\right| \geq s\right) \leq \exp\left(-\frac{ns^2}{2}\right).$$

Note that

$$\tilde{h}_m = (2m(\ln(m+1) - \ln \gamma))^{1/2}.$$

At step  $s$ , if the process does not stop, it implies that

$$\sum_{i=1}^s \tilde{Z}_i(\theta)/s \leq \tilde{h}_s/s.$$

Let  $\tau_0$  be the threshold such that

$$\tilde{h}_\tau/\tau \leq c\varepsilon^\kappa/2, \quad \forall \tau \geq \tau_0.$$

Set  $\tau^\uparrow(\delta, \varepsilon) = \max\{\tau_0, \frac{8 \log(1/\delta)}{c^2 \varepsilon^{2\kappa}}\} = \tilde{O}(\varepsilon^{-2\kappa})$ . Then we have

$$\begin{aligned} & \mathbb{E}[\mathbf{1}(|\theta - \theta^*| > \varepsilon) \mathbf{1}(T^\uparrow(\theta) \geq \tau^\uparrow(\delta/2, \varepsilon))] \\ & \leq \mathbb{E}[\mathbf{1}(|\theta - \theta^*| > \varepsilon) \mathbf{1}(T^\uparrow(\theta) \geq \tau^\uparrow(\delta/2, \varepsilon)) \mathbf{1}(\mathcal{E})] + \mathbb{P}(\mathcal{E}^c) \\ & \leq \mathbb{E}[\mathbf{1}(2\tilde{p}(\theta) - 1 \geq c\varepsilon^\kappa) \mathbf{1}(T^\uparrow(\theta) \geq \tau^\uparrow(\delta/2, \varepsilon))] + \frac{1}{2}\delta \\ & \leq \mathbb{E}\left[\mathbf{1}(2\tilde{p}(\theta) - 1 \geq c\varepsilon^\kappa) \mathbf{1}\left(\sum_{i=1}^{\tau^\uparrow(\delta/2, \varepsilon)} \tilde{Z}_i(\theta)/\tau^\uparrow(\delta/2, \varepsilon) \leq \tilde{h}_{\tau^\uparrow(\delta/2, \varepsilon)}/\tau^\uparrow(\delta/2, \varepsilon)\right)\right] + \frac{1}{2}\delta \\ & \leq \mathbb{E}\left[\mathbf{1}(2\tilde{p}(\theta) - 1 \geq c\varepsilon^\kappa) \mathbf{1}\left(\sum_{i=1}^{\tau^\uparrow(\delta/2, \varepsilon)} \tilde{Z}_i(\theta)/\tau^\uparrow(\delta/2, \varepsilon) \leq c\varepsilon^\kappa/2\right)\right] + \frac{1}{2}\delta \\ & \leq \mathbb{P}\left(\left|\sum_{i=1}^{\tau^\uparrow(\delta/2, \varepsilon)} \tilde{Z}_i(\theta)/\tau^\uparrow(\delta/2, \varepsilon) - (2\tilde{p}(\theta) - 1)\right| \geq c\varepsilon^\kappa/2\right) \leq \exp\left(-\frac{\tau^\uparrow(\delta/2, \varepsilon)c^2\varepsilon^{2\kappa}}{8}\right) + \frac{1}{2}\delta \leq \delta, \end{aligned}$$

where the last inequality holds because  $\tau^\uparrow(\delta/2, \varepsilon) \geq \frac{8 \log(2/\delta)}{c^2 \varepsilon^{2\kappa}}$ .  $\square$

*Proof of Theorem 4.* First, we decompose the moves to Phase I and Phase II as follows

$$\begin{aligned} \mathbb{E}\left[\sum_{k=1}^{T^\rightarrow} T^\uparrow(\theta_k)\right] &= \mathbb{E}\left[\sum_{k=1}^{T^\rightarrow} T^\uparrow(\theta_k) \mathbf{1}(\|\theta_k - \theta^*\| \geq a)\right] + \mathbb{E}\left[\sum_{k=1}^{T^\rightarrow} T^\uparrow(\theta_k) \mathbf{1}(\|\theta_k - \theta^*\| \leq a)\right] \\ &\leq \mathbb{E}\left[\sum_{k=1}^{\psi(a)} T^\uparrow(\theta_k) \mathbf{1}(\|\theta_k - \theta^*\| \geq a)\right] + \mathbb{E}\left[\sum_{k=1}^{T^\rightarrow} T^\uparrow(\theta_k) \mathbf{1}(\|\theta_k - \theta^*\| \leq a)\right]. \end{aligned}$$

Proposition 3 gives that

$$\mathbb{E} \left[ \sum_{k=1}^{\psi(a)} T^\uparrow(\theta_k) \mathbf{1}(\|\theta_k - \theta^*\| \geq a) \right] \leq \left( \frac{4\theta^*}{r_2\alpha a} + \frac{4\beta_1}{r_1} + \frac{2\beta_2}{r_R} \right) \max_{a \leq \|\theta - \theta^*\| \leq \tau} \phi(\tilde{p}(\theta)). \quad (\text{A.6})$$

There are two stopping criteria for Algorithm 2: 1) the horizontal move reaches  $\tau^\rightarrow(\delta, \varepsilon)$ ; or 2) the horizontal move reaches  $\tau^\rightarrow(\delta/2, a)$  and the vertical move reaches  $\tau^\uparrow(\delta/2, \varepsilon)$ . In both cases, we have the number of moves bounded by  $\max\{\tau^\rightarrow(\delta, \varepsilon), \tau^\rightarrow(\delta/2, a)\}\tau^\uparrow(\delta/2, \varepsilon)$ . Therefore,

$$\mathbb{E} \left[ \sum_{k=1}^{T^\rightarrow} T^\uparrow(\theta_k) \mathbf{1}(\|\theta_k - \theta^*\| \leq a) \right] \leq \tau^\rightarrow(\delta/2, \varepsilon)\tau^\uparrow(\delta/2, \varepsilon). \quad (\text{A.7})$$

Thus, combining (A.6) and (A.7), we have

$$\mathbb{E} \left[ \sum_{k=1}^{T^\rightarrow} T^\uparrow(\theta_k) \right] \leq \left( \frac{4\theta^*}{r_2\alpha a} + \frac{4\beta_1}{r_1} + \frac{2\beta_2}{r_R} \right) \max_{a \leq \|\theta - \theta^*\| \leq \tau} \phi(\tilde{p}(\theta)) + \max\{\tau^\rightarrow(\delta, \varepsilon), \tau^\rightarrow(\delta/2, a)\}\tau^\uparrow(\delta/2, \varepsilon). \quad \square$$

*Proof of Theorem 6.* Theorem 5 states that  $s$ -dimensional important features can be correctly identified with probability at least  $1 - \delta$  when the noisy labeled data is more than  $H_0(\delta, \varepsilon; \underline{\beta}_\Theta)$ . Combined with Theorem 4, we reach our conclusion.  $\square$

## A.2. Proofs in Section 4

Before proving Theorem 5, we first show the following result. It proves that when the  $\ell_\infty$ -curvature condition holds,  $\|\frac{1}{n}(\mathbf{X}_S^\top \mathbf{X}_S)^{-1}\|_\infty$  can also be bounded.

LEMMA 8. *For any  $\mathbf{X}$ , if it satisfies that*

$$\left\| \frac{1}{n} \mathbf{X}^\top \mathbf{X} z \right\|_\infty \geq \gamma \|z\|_\infty \text{ for all } z \in C_\alpha(S),$$

*then we have*

$$\left\| \frac{1}{n} (\mathbf{X}_S^\top \mathbf{X}_S)^{-1} \right\|_\infty \leq \frac{1}{\gamma}.$$

*Proof of Lemma 8.* We first note that for all matrix  $A$ ,

$$\|A^{-1}\|_\infty = \frac{1}{\min\{\|Ax\|_\infty : \|x\|_\infty = 1\}}. \quad (\text{A.8})$$

For any  $z_S$  such that  $\|z_S\|_\infty = 1$ , we let  $z_{S^c} = 0$  and  $z = (z_S, z_{S^c}^c)$ . It is obvious that  $z \in C_3(S)$ , so according to the condition,

$$\left\| \frac{1}{n} \mathbf{X}_S^\top \mathbf{X}_S z_S \right\|_\infty = \left\| \frac{1}{n} \mathbf{X}^\top \mathbf{X} z \right\|_\infty \geq \gamma \|z\|_\infty = \gamma.$$

From Equation (A.8), we have

$$\left\| \frac{1}{n} (\mathbf{X}_S^\top \mathbf{X}_S)^{-1} \right\|_\infty \leq \frac{1}{\gamma}. \quad \square$$

Now we are ready to prove Theorem 5.

*Proof of Theorem 5.* Corollary 7.22 in [Wainwright \(2019\)](#) states that for any matrix  $\mathbf{X}$  that satisfies Assumption 5(II) (lower eigenvalue) and (I) (mutual incoherence), then it satisfies the  $\ell_\infty$ -error bound

$$\|\hat{\theta}_S - \theta_S^*\|_\infty \leq \frac{\sigma}{\sqrt{c_{\min}}} \left\{ \sqrt{\frac{2 \log s}{n}} + \zeta \right\} + \left\| \left( \frac{\mathbf{X}_S^\top \mathbf{X}_S}{n} \right)^{-1} \right\|_\infty \lambda_n, \quad (\text{A.9})$$

with probability at least  $1 - 4e^{-n\zeta^2/2}$ . From Lemma 8, it states that the  $\ell_\infty$ -curvature condition implies that

$$\left\| \frac{1}{n} (\mathbf{X}_S^\top \mathbf{X}_S)^{-1} \right\|_\infty \leq \frac{1}{\alpha_2}. \quad (\text{A.10})$$

Substituting (A.10) into (A.9), we conclude that

$$\|\hat{\theta}_S - \theta_S^*\|_\infty \leq \frac{\sigma}{\sqrt{c_{\min}}} \left\{ \sqrt{\frac{2 \log s}{n}} + \zeta \right\} + \frac{1}{\alpha_2} \lambda_n.$$

Theorem 7.21 in [Wainwright \(2019\)](#) also implies no false inclusion. Thus we reach our conclusion.  $\square$

*Proof of Proposition 4.* First, if only utilizing Lasso for the supervised learning oracle to refine the estimator based on  $n$  noisy labeled data, subject to certain regularity conditions, the estimation error can be bounded as  $\|\hat{\theta}_n - \theta^*\|_2 \leq c\sigma\sqrt{s \log d/n}$  with high probability for some constant  $c > 0$  ([Wainwright 2019](#)). Equivalently, to ensure that the two-norm distance of the estimation error is within  $\varepsilon$ , we need to acquire  $O(\sigma^2 s \log d/\varepsilon^2)$  data points. Theorem 6 implies that for sufficiently small  $\varepsilon$ , the sample complexity scales with  $s^{1+\kappa}/\varepsilon^{2\kappa}$ .

By comparing two terms, we have the condition of 3 performing better than SFT (ignoring the logarithm term) as

$$\frac{\sigma^2}{s^\kappa} \gtrsim \varepsilon^{2-2\kappa}.$$

$\square$

## Appendix B: Additional Results

### B.1. Numerical illustrations for Example 3

In this experiment, each coordinate of  $X_i \in \mathbb{R}^{1000}$  is generated from Gaussian distribution with mean 0 and standard deviation 100. To reflect our sparse setup, we set  $\theta_1 = -0.5$ ,  $\theta_2 = 5$ , and the remaining coefficients to 0. The observational noise follows Gaussian distribution with mean 0 and standard deviation 200. By training on a dataset comprising 2000 data points, we obtained estimated parameter  $\hat{\theta}_1 = 0.47$  and  $\hat{\theta}_2 = 5.87$ . It is noteworthy that the estimated sign of the first parameter is incorrect, indicating a potential issue in pure supervised learning.

### B.2. Details about $\kappa$

We explain why it is natural to assume  $\kappa \leq 1$ . When collecting  $B$  noisy data points to make the comparison between two models  $y = (\theta + \Delta)x + \epsilon$  and  $y = (\theta - \Delta)x + \epsilon$ , where the noise follows Gaussian distribution



with mean 0 and standard deviation  $\sigma$ , we have the probability of model parameter  $\theta + \Delta$  more preferable than  $\theta - \Delta$  as

$$\begin{aligned}
\mathbb{P}(\theta + \Delta \succeq \theta - \Delta) &= \mathbb{P}\left(\sum_{i=1}^B (\theta^* x + \epsilon_i - (\theta + \Delta)x)^2 \leq \sum_{i=1}^B (\theta^* x + \epsilon_i - (\theta - \Delta)x)^2\right) \\
&= \mathbb{P}\left(\frac{1}{B} \sum_{i=1}^B \epsilon_i \geq (\theta - \theta^*)|x|\right) \\
&= \int_{-\infty}^{(\theta^* - \theta)|x|} \frac{\sqrt{B}}{\sigma\sqrt{2\pi}} e^{-\frac{1}{2}(z\sqrt{B}/\sigma)^2} dz \\
&= \frac{1}{2} + \frac{\sqrt{B}}{\sigma\sqrt{2\pi}} \int_0^{(\theta^* - \theta)|x|} e^{-\frac{1}{2}(z\sqrt{B}/\sigma)^2} dz \\
&\geq \frac{1}{2} + \frac{\sqrt{B}}{\sigma\sqrt{2\pi}} \int_0^{(\theta^* - \theta)|x|} \left(1 - \frac{1}{2}B(z/\sigma)^2\right) dz \\
&= \frac{1}{2} + \frac{\sqrt{B}}{\sigma\sqrt{2\pi}} \left( (\theta^* - \theta)|x| - \frac{B((\theta^* - \theta)|x|)^3}{6\sigma^2} \right) \\
&= \frac{1}{2} + \sqrt{B}\Omega((\theta^* - \theta)|x|).
\end{aligned}$$

□